Neurogenetic Analysis of *C. elegans* Developmental Decision-making

Thesis by

Cynthia Mei-Ling Chai

In Partial Fulfillment of the Requirements for

the degree of

Doctor of Philosophy

CALIFORNIA INSTITUTE OF TECHNOLOGY

Pasadena, California

2021

(Defended 10th May 2021)

ACKNOWLEDGEMENTS

The Road goes ever on and on
Down from the door where it began.
Now far ahead the Road has gone,
And I must follow, if I can,
Pursuing it with eager feet,
Until it joins some larger way
Where many paths and errands meet.
And whither then? I cannot say.

- J.R.R. Tolkien, The Lord of the Rings: The Fellowship of the Ring

In just eight lines, Tolkien captured the essence of life in academic science. I've had this verse tacked above my lab bench since the start of graduate school. It provided much-needed perspective at critical moments.

The Road of graduate school is decidedly more enjoyable when your advisor is the inimitable Paul Sternberg. Ever supportive and always armed with a funny anecdote, his willingness to grant me my creative freedom and independence is the main reason I've not just survived but also thrived as a student scientist.

Sometimes a pit stop at a Roadside tavern is necessary to get directions when uncertain about the way forward. My committee members Joe, David, and Marianne are the steadfast innkeepers who've seen it all and readily impart their wisdom.

On the Road, you'll meet fellow battle-weary travelers with whom you can commiserate over greasy takeout. My labmates and friends at Caltech have fulfilled this vital role. Sometimes you even discover that joining forces is the path of most productivity. Thus, a mutually-beneficial scientific collaboration is born.

Like many international scientists, I've had to leave my family half a world away to complete my quest. Thank goodness this realm is more technologically advanced than Middle-earth and video calls are available to close the distance.

Finally I want to thank all the Gandalfs who encouraged me to undertake this journey in the first place. They saw something in me that I couldn't yet see in myself. Maybe it was magic, but I'm more inclined to call it good mentorship.

ABSTRACT

How does the neuronal genome dictate cellular physiology and function, which in turn impacts organismal development? This is the central question driving all the projects in this thesis. Here, we leveraged the well-defined nervous system and genetics of *Caenorhabditis elegans* to apply this genes to neurons to phenotype experimental approach. In Chapter 2, we delineate how a pair of first order amphid interneurons integrates conspecific cues and propagates this information via neuropeptidergic pathways to influence larval developmental fate. In Chapter 3, we identify and characterize a role for the evolutionarily-conserved forkhead transcription factor FKH-7/FOXP in regulating sensory neuron function during developmental decision-making. Our results show that perturbations of single genes encoding transcription factors, neuropeptides, and receptors can significantly alter neuronal function and ultimately have profound effects on an organism's life history.

for Mum, Dad, and my brother

Because of them, I have the courage to wander and am never lost.

TABLE OF CONTENTS

Chapter 1: Introduction

1.1 *Caenorhabditis elegans* overview

C. elegans growth and maintenance

Caenorhabditis elegans is a microscopic, free-living nematode that can be easily cultured in the laboratory on agar-filled petri dishes seeded with the non-pathogenic *Escherichia coli* OP50 strain as a food source[1]. Healthy *C. elegans* can be cultured at temperatures ranging from 15°C to 25°C, although 20-22°C is the range used for most experiments. Although *C. elegans* has two sexes, it is most frequently found in its hermaphroditic form. Hermaphrodites have five pairs of autosomal chromosomes and two sex chromosomes while males have five pairs of autosomal chromosomes and one sex chromosome[1]. The ability of hermaphrodites to self-fertilize and generate self-progeny of invariant genetic backgrounds simplifies routine animal maintenance procedures. When cross-progeny are required, however, hermaphrodites can be easily mated with males.

Anatomically, *C. elegans* has many of the tissue types that are also found in mammals including muscle, hypodermis, intestine, and neurons. Food is sucked into the pumping pharynx where it is ground into smaller particles and passed into the intestinal lumen for nutrient extraction (Figure 1). *C. elegans* has a cylindrical body shape and asymmetric body wall muscle activation generates undulatory locomotion on two-dimensional surfaces. Its transparent hypodermis is the cornerstone of *C. elegans'* utility as a model organism in basic research, enabling the visualization of *in vivo* processes at cellular resolution in post-embryonic whole mount samples. The nervous system is small but specialized enough to control a wide range of behavioral and physiological processes. *C. elegans* also displays sexual dimorphism with regards to tissue structure and function. Males have a specialized tail structure that enables them to copulate with hermaphrodites[2]. They also have a larger number of neurons presumably to accommodate their expanded mating-related repertoire of behaviors[3].

The *C. elegans* nervous system

The adult hermaphrodite nervous system has 302 neurons and the synaptic connections between them have been fully mapped (Figure 2)[3]. Neuronal cell bodies are largely clustered in head and tail ganglia, with synaptic connections most densely

concentrated in the nerve ring in the head. These 302 neurons can be further subdivided into 118 neuron classes based on topology and synaptic connectivity. The majority of neuron classes comprise bilaterally symmetrical pairs. Another dimension of neuron sub-classification relates to their circuitry by which neurons are grouped as either sensory neurons, interneurons, motor neurons, or polymodal neurons. Sensory neurons have morphological specializations such as dendritic projections that interface with the external environment and bipolar morphologies that enable them to transmit these inputs to other neurons in the nerve ring. Interneurons are monopolar or bipolar and receive synapses from other neurons and transmit this information to other neurons. Motor neurons are characterized by their direct synaptic connections onto muscle cells. Polymodal neurons fulfill more than one of the previous three descriptions.

The structure and function of *C. elegans'* chemosensory apparatus has been intensively studied. Chemosensory neurons enable the worm to taste and smell their environment by detecting soluble chemical cues and airborne odorants respectively. Chemosensory neurons can be found in both the amphid structures in the head and the phasmid structures in the tail (Figure 3). Ultimately, all axonal projections originating from amphid and phasmid sensory neurons come into close proximity with each other and those of other neurons within the nerve ring that wraps around the pharynx (Figure 2). The dendritic endings of many amphid chemosensory neuron classes have unique morphologies which facilitates rapid identification in transgenic reporter animals (Figure 4). In addition to chemical stimuli, *C. elegans* is also able to sense touch, light, and temperature[4–6].

The *C. elegans* neuronal genome

302 neurons is considerably smaller than the 100 000 neurons in flies and 75 million neurons in mice. However, the *C. elegans* nervous system is simple only in this numerical sense. Invertebrate genomes have undergone two duplication events on the way to vertebrates. Thus, a one-to-four gene ortholog relationship between *C. elegans* and vertebrates is expected. For many gene families with neuron-specific functions, however, this is often not the case[7]. Two pore TWK potassium channels, Cys-loop ligand-gated ion channels, and chloride channels are a few examples of neuronal gene families which have

undergone substantial expansion in *C. elegans* that are directly involved in setting cell membrane potential[7]. Furthermore, different spatiotemporal expressions of this nematode-specific suite of expanded neuronal gene families can enable a single *C. elegans* neuron class to perform multiple processing functions in a context-specific manner.

With their structurally compact yet molecularly diverse system, the worm is able to sense and react to a wide variety of external stimuli. This is further aided by the action of neuropeptides, which are secreted by diverse tissues and bind to their cognate G-protein coupled receptors (GPCRs) to modulate the activity of neurons. The *C. elegans* genome is predicted to encode 153 neuropeptide GPCRs, although there are many orphan chemoreceptor GPCRs and ligand-gated ion channels that might also be involved in neuropeptide signaling[7–10]. The combinatorial binding of neuropeptides to differentially-expressed GPCRs provides an additional layer of neural signaling networks on top of the hard-wired connectome, vastly expanding the repertoire of physiological and behavioral processes that can be controlled by a limited number of neurons. Thus, *C. elegans* provides the ideal experimental arena in which to identify and mechanistically dissect neurogenetic regulatory motifs at the molecular and cellular level.

There are some interesting differences in information propagation mechanisms between vertebrate and *C. elegans* neurons. The *C. elegans* neuronal genome does not encode voltage-gated sodium channels and membrane depolarization is driven by voltage-gated calcium channels. The neurotransmitter identity of different neuron classes has been fully mapped in *C. elegans*. Acetylcholine and glutamate are the main neurotransmitters in the *C. elegans* nervous system with 52 cholinergic neuron classes and 38 glutamatergic neuron classes[11,12]. An interesting motif that has arisen from this neurotransmitter atlas is that most *C. elegans* sensory neurons are glutamatergic while the majority of interneurons are cholinergic[11]. Although GABA is the main inhibitory neurotransmitter in vertebrate nervous systems, only 6 neuron classes are GABAergic in *C. elegans*[13]. This doesn't necessarily mean that *C. elegans* circuits primarily use postsynaptic neuron activation in their computations. *C. elegans* neuron classes can also express ionotropic glutamate-gated chloride channels like those encoded by the invertebrate-specific *glc* family as well as the inhibitory metabotropic glutamate receptor-encoding *mgl-1*[14]. In addition, cholinergic

neurotransmission in *C. elegans* can be inhibitory due to the expression of the ACC acetylcholine-gated chloride channels[15]. The *acc* gene family has no orthologs in vertebrate genomes[15]. Thus, it is clear that our understanding of relationships between synaptic connections and organismal phenotypes will be significantly enriched through interpretation in light of the above features of the *C. elegans* neuronal genome.

1.2 Mechanisms of *C. elegans* diapause entry

Intraspecific variation arises from either polymorphisms or polyphenisms, both of which differ in their sources of phenotypic variation. While polymorphisms refer to genetic changes that give rise to alternative phenotypes, polyphenisms are the result of environmental variability. Developmental plasticity is the ability of a single genotype to produce alternative developmental phenotypes in response to different environments. Adaptive developmental plasticity endows the organism with behavioral, physiological, and/or morphological traits that enhances its later life ecological success in the selective environment. This adaptive strategy is pervasive in nature and often results in long-lasting changes such as switches in developmental trajectories that irreversibly alter the adult phenotype. Examples of this include seasonal wing pattern differences in *Bicyclus* butterflies[16,17], protective helmet development in *Daphnia* in response to predator cues[18], and increased later life health risks in humans due to *in utero* malnourishment[19]. In some cases, developmental plasticity takes the form of reversible arrested states as in the case of killifish embryos exposed to drought conditions[20,21] or parasitic nematode infective juveniles when challenged with resource scarcity[22]. Developmental plasticity can result from either direct or indirect effects of the environment. In the former case, the environmental cue directly impinges upon physiological processes such as the effect of high temperatures on chemical reaction kinetics or developmental processes such as low body weight as a result of prolonged starvation, and can be non-adaptive[23]. On the other hand, indirect effects involve inductive cues that are predictive of and distinct from the future selective environment. For example, high levels of conspecific-secreted pheromone and low food availability induces *C. elegans* diapause entry and results in the dauer stage phenotype that is highly adapted to survive the oncoming bust conditions[24].

The alternative diapause life cycle

Under optimal growth conditions, *C. elegans* has a life cycle of three days during which it undergoes four successive larval molts post-hatching (Figure 5)[25]. When environmental conditions are deleterious, however, larvae can enter a stress-resistant alternate developmental stage called the dauer stage[26]. The decision to enter diapause is an

anticipatory one that is made when the environment's suitability for future reproductive growth is deemed to be low. Entry into the diapause developmental trajectory is triggered by detection of high conspecific-secreted pheromone concentrations, high temperatures, and low food availability[27]. Under these conditions, L1 stage larvae will first enter the preparatory pre-dauer L2d stage (Figure 5)[27]. If these adverse conditions persist during L2d, larvae will make a second decision to commit to forming dauer larvae as opposed to re-entering the reproductive trajectory as L3 larvae (Figure 5)[27]. Should external conditions improve, dauer larvae can exit diapause and re-enter the reproductive trajectory as L4 larvae (Figure 5)[27].

Interestingly, pheromone concentrations that ultimately yield low percentages of dauers is sufficient to induce all L1 larvae to enter the pre-dauer L2d stage[27]. This indicates that the initial L1 decision to enter L2d might serve as a hedging strategy that buys the larvae more time to sample its surrounding environment before fully committing to either developmental fate. Transitioning into and out of diapause is metabolically costly as it requires multi-tissue remodeling (see next section). Coupled with the potential loss of nutritional and reproductive opportunities while in the arrested state, an ill-judged decision to enter diapause can be maladaptive. By shifting larvae from unfavorable to favorable growth conditions at different developmental time points, commitment to the dauer fate under pheromone-inducing conditions was determined to occur only at the mid-point of the L2d stage[28]. The additional sampling time provided by entering the preparatory L2d stage is advantageous because natural cues are often noisy and a longer period of evidence accumulation could minimize decision-making errors.

Adaptive changes during the dauer stage

Dauer larvae possess several adaptions that enable them to survive, endure, and escape adverse environmental conditions. In this developmentally-arrested stage, larvae are radially constricted and develop a thickened cuticle that has characteristic longitudinal ridges called alae (Figure 6)[26]. They also develop a buccal plug that seals off their mouth opening and are non-feeding throughout this life stage[26,29]. Germline proliferation is arrested during diapause and accumulated body fat stores are visible as enlarged intestinal lipid droplets (Figure 6)[30,31]. Extensive structural remodeling of the nervous system also occurs such as

dendritic arborization of the inner labial IL2 ciliated neurons, a numerical increase in AFD thermosensory neuron distal tip microvilli, and enlargement of the AWC olfactory neuron ciliated wings[29,32]. However, the functional contributions of these structural changes to dauer-specific behaviors has not been established. Although rewiring of chemical synapses in dauers has been hypothesized, this has yet to be probed with EM reconstruction. Recent studies have revealed expression changes in genes encoding neuropeptides, innexins, and chemoreceptors that contribute to dauer-specific nervous system connectivity and function[33–36]. This stage-dependent plasticity of the neuronal genome confers dauer-specific behaviors such as nictation and carbon dioxide attraction[37,38]. These dauer-specific behaviors presumably facilitate dispersal strategies to more bountiful habitats by enabling host seeking.

The chemical composition of dauer-inducing pheromone

Dauer-inducing pheromone is a mixture of hydrophilic dideoxy sugar ascarylose derivatives called ascarosides that can be differentiated based on the lengths of their carbon side chains and additional side groups. These secreted metabolites serve as a proxy for high conspecific density and competition for limited resources in the local area. The dauer-inducing ability of pheromone extract was first identified and described by Golden and Riddle in 1982[24]. Since then, the ascaroside composition of crude pheromone extracts has been analyzed using activity guided fractionation, NMR spectroscopy-based, and mass spectrometry-based comparative metabolomics[39–43]. The first ascaroside component of dauer-inducing pheromone to be isolated and characterized was ascr#1 (also called "daumone")[41]. However, concentrations of ascr#1 that were much higher than that found in pheromone extract and toxic to non-arrested animals were required to induce diapause entry[41,44]. Thus, ascr#1 activity alone could not account for the potent dauer-inducing effects of crude pheromone extract indicating that pheromone must also comprise other active components. Further identification of other ascarosides followed by experiments using various combinations of these synthetic ascarosides revealed both additive and synergistic relationships between different ascarosides in the context of dauer formation[39,40,43,45,46]. In addition, dimerization between G-protein coupled chemoreceptors can be essential for their function as in the case of the ascr#2-sensing DAF-37 and DAF-38 receptor complex[47]. Thus,

a complex signaling network comprised of interacting ascaroside chemoreceptors expressed by different amphid sensory neurons collectively encode the secreted conspecific signal that influences developmental fate. The vastness and diversity of the *C. elegans* chemoreceptor repertoire has precluded systematic screens for chemoreceptor function and perhaps as a result of that, the number of functionally validated ascaroside-chemoreceptor pairings in the current literature remains small[48–51]. A study surveying ascaroside secretions from free-living and parasitic nematode species showed that ascaroside mixtures have species-specific compositions in terms of chemical structures and relative ratios[52]. Based on this, it is plausible that the ascaroside signaling code influencing dauer formation might be species-specific as well. In one example, *Pristionchus pacificus* pheromone extract does not induce *C. elegans* dauer formation and vice versa[53]. However, more species pairings across different clades and lifestyles need to be examined before drawing generalizable conclusions about this relationship.

Neuroendocrine signaling pathways

The evolutionarily-conserved DAF-7/TGF-ß and insulin signaling pathways are the two main endocrine pathways regulating *C. elegans* dauer formation. *daf-7* is specifically expressed in the ASI amphid chemosensory neurons and *daf-7* loss of function mutants have a dauer constitutive phenotype indicating that DAF-7 promotes reproductive growth[54,55]. Consistent with this, dauer pheromone exposure and starvation conditions downregulate ASI *daf-7* expression[54,55]. Rigorous genetic dissection of the DAF-7/TGF-ß pathway has identified downstream molecular mediators and proposed the following model. Under favorable growth conditions, DAF-7/TGF-ß secreted by the ASI neurons binds to type I and type II serine/threonine kinase receptors encoded by *daf-1* and *daf-4*[56,57]. Receptor activation promotes translocation of DAF-8 and DAF-14 SMAD proteins into the nucleus where they inhibit the DAF-3/SMAD and DAF-5/SNO-SKI complex and activate reproductive growth-promoting transcriptional programs[58–61].

The insulin-like neuropeptide *ins* gene family has 38 members which bind to the widely-expressed DAF-2, the only member of the insulin receptor family in C. elegans[62,63]. Different insulin neuropeptides can act as either agonists and antagonists of the DAF-2

receptor suggesting that combinatorial binding of ligands from different sources might play a role in the complex dauer formation process[62,64]. Similar to the reproductive growth-promoting DAF-7/TGF-ß, *daf-2* loss of function mutants display a dauer constitutive phenotype[65]. Further genetic analysis has revealed that the forkhead transcription factor DAF-16/FOXO is downstream of DAF-2 in the insulin signaling pathway and that signaling via DAF-2 antagonizes DAF-16's dauer formation-promoting effects[66,67]. Under favorable growth conditions, activation of DAF-2 increases PIP_3 production via activation of the AGE-1/PI3K kinase[68]. The presence of both PIP_3 and PDK-1 kinase results in phosphorylation of DAF-16 by the AKT-1/2 and SGK kinase complex preventing translocation of DAF-16 into the nucleus[69–74]. Under unfavorable dauer-inducing conditions, unphosphorylated DAF-16 enters the nucleus where it activates transcriptional programs responsible for enhancing stress-resistance and promoting dauer formation.

Sensory control of diapause entry

A young larva's sensory perception of external environmental conditions triggers the diapause entry decision. Three environmental cues have been associated with the diapause entry decision – pheromone, food, and temperature[27]. The *C. elegans* nervous system interfaces with its chemical environment through the exposed ciliated dendritic endings of the amphid (head) and phasmid (tail) chemosensory neurons. Indeed, many cilium structure mutants exhibit dauer formation phenotypes as a result of global chemosensory defects[75–77]. The roles of all eleven amphid chemosensory neuron classes in dauer formation have been examined either through laser or genetic ablation. Three classes were found to inhibit diapause entry (ADF, ASI, ASG) while three more promoted diapause entry (ASK, ADL, ASJ)[49,55,78]. The relative contributions of individual sensory neuron classes to the diapause entry decision can vary depending on growth conditions. For example, ASK ablation dramatically reduces dauer formation when grown under ascaroside dauer-inducing conditions but not under normal culturing conditions[49,78]. This indicates that the ascaroside signal detected by ASK interacts with inputs from other sensory neuron classes to control the developmental decision. Furthermore, synaptic connectivity between the six chemosensory neuron classes with reported roles in dauer formation is sparse indicating that multimodal

inputs relevant to diapause entry might be integrated outside the sensory layer[3]. However, the neural basis of this integrative process downstream of sensory signaling has not been explored. This highlights a wider issue in the field of developmental plasticity where the mechanisms linking environmental perception and terminal neuroendocrine signaling pathways that enact the developmental phenotype remain largely uncharacterized.

1.3 Summary of Findings

Phenotypic plasticity is a pervasive adaptive strategy in nature that is guided by an organism's sensory perception of prevailing environmental conditions. Unlike behavioral plasticity, the alternative phenotypes resulting from developmental plasticity is enacted over longer timsescales which often makes it difficult to apply integrative approaches to dissect its neural and molecular underpinnings. Thus, although it is known that sensory cues are integrated in an animal's brain and the resulting developmental fate decision is executed by terminal neuroendocrine pathways, *how* this integration occurs is less clear.

In Chapter 2, we leveraged the well-defined nervous system and genetics of *C. elegans* to investigate the mechanisms behind this integrative process in the context of the *C. elegans* larval diapause entry decision. We combine pharmacological neuron silencing, genetic epistasis analysis, and functional imaging to reveal how a pair of interneurons integrates pheromone cues and transduces this information into neuropeptidergic pathways that orchestrate larval developmental fate.

The quality and efficacy of an animal's decision is contingent upon the accuracy of their sensory perception. In Chapter 3, we discover a novel role for the previously unstudied *C. elegans* forkhead transcription factor FKH-7 in regulating sensory neuron function during the diapause entry decision. FKH-7 is the sole worm ortholog of the FoxP subfamily of transcription factors, which have been implicated in multiple cognitive developmental disorders. We find that autism spectrum disorder-associated *fkh-7* missense variants are also defective in developmental decision-making paving the way for interrogation of disease-relevant signaling pathways using this paradigm.

By perturbing single genes/neurons and studying their impact at the organismal level, we provide insights into the 'black box' of decision-making mechanisms that underlie developmental plasticity.

1.4 Figures

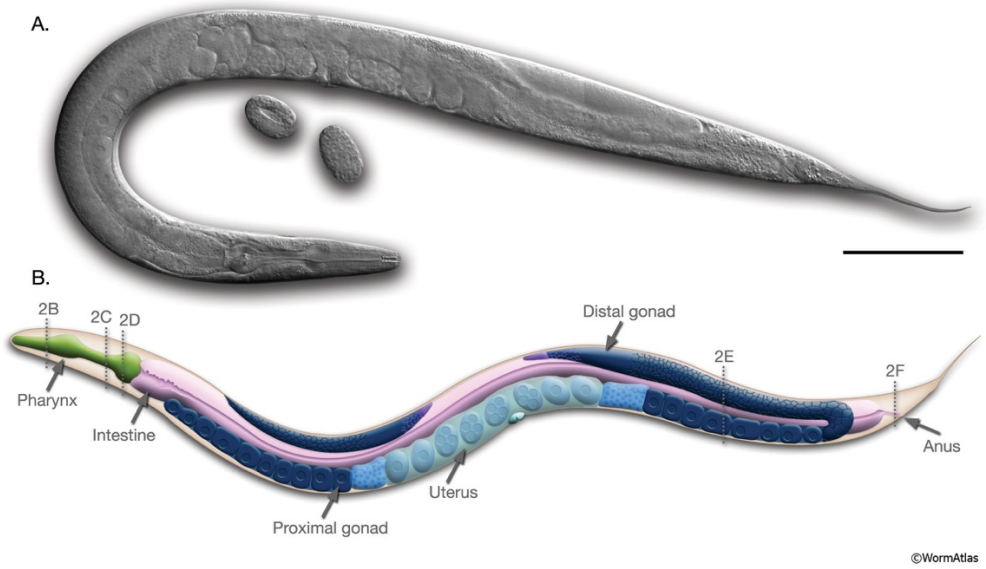

Figure 1: Anatomy of an adult hermaphrodite.

(A) DIC image of an adult hermaphrodite, left lateral side. Scale bar 0.1 mm.

(B) Schematic drawing of anatomical structures, left lateral side.

(Unmodified figure from WormAtlas.[79])

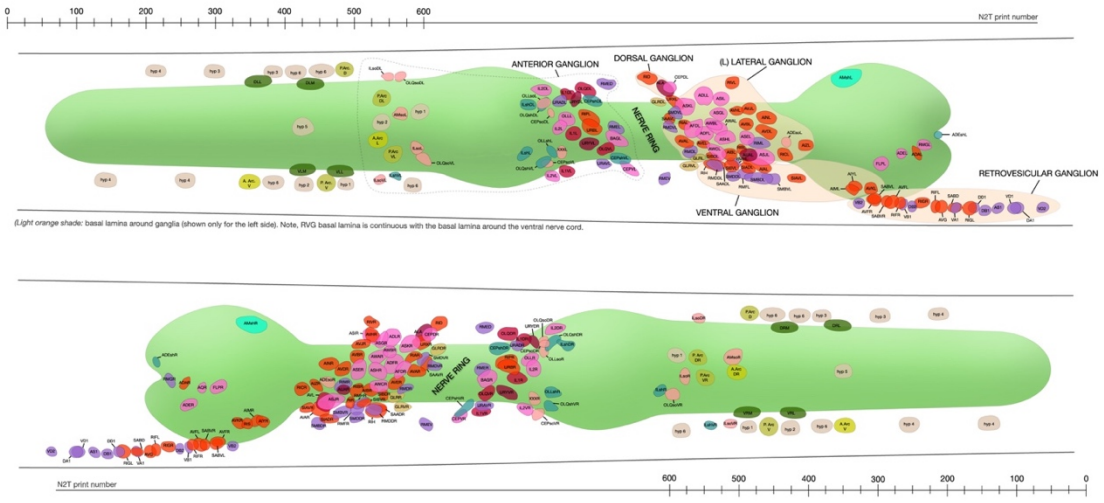

Figure 2. Schematic showing the locations of neuronal cell bodies and their associated cells in the head is shown in left-hand (a) and right-hand (b) views. Pharynx is colored green. (Unmodified figure from WormAtlas.[79])

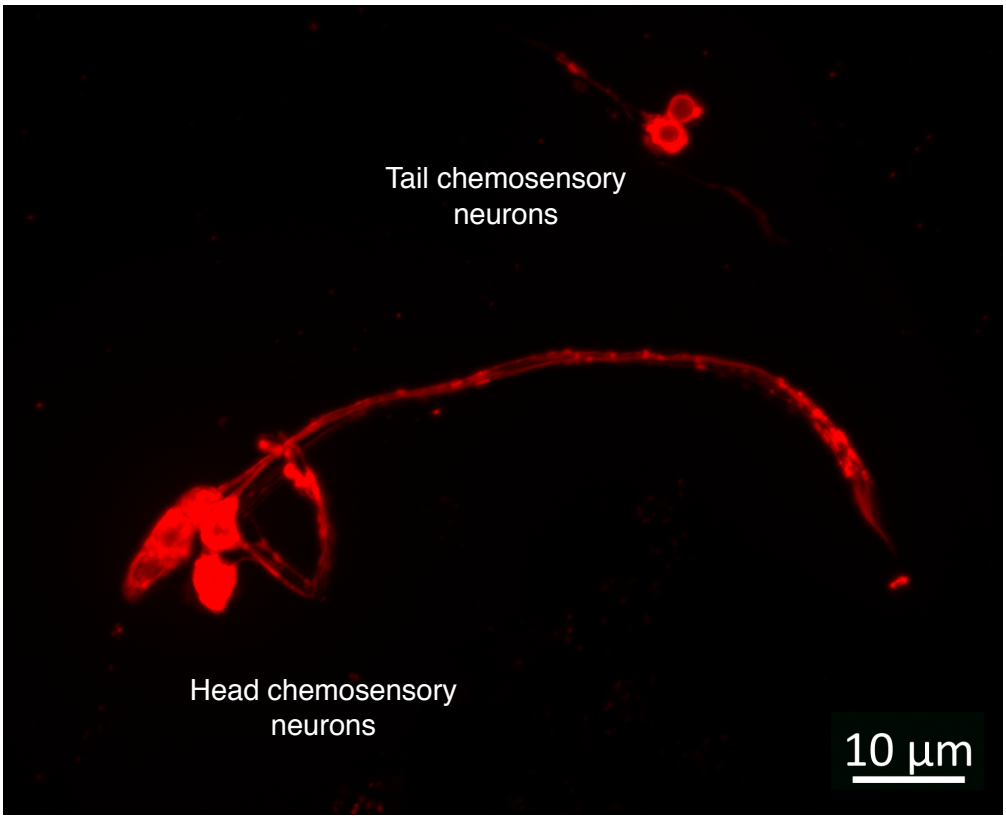

Figure 3. A subset of amphid (head) and phasmid (tail) chemosensory neurons. L1 stage larva stained with lipophilic DiI dye.

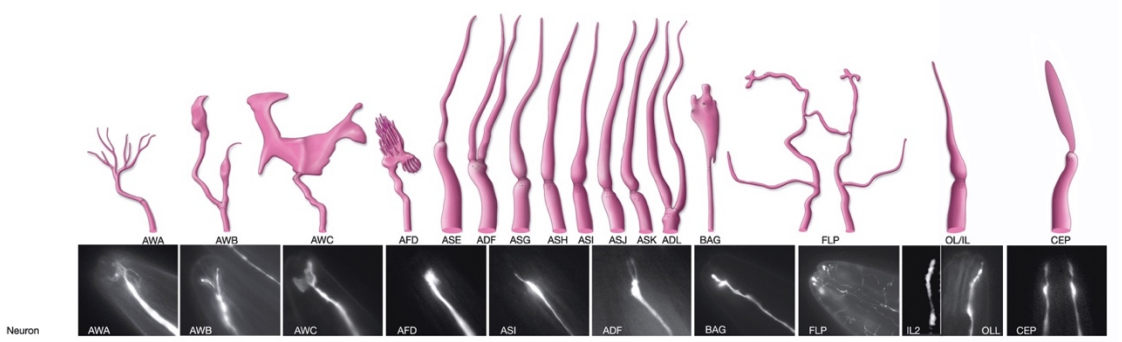

Figure 4: Cilia morphology of the sensory neurons that terminate in the lips. (*Top panel*) Illustrations of cilia. (*Bottom panel*) Epifluorescent images of cilia (OLQ and IL1 are not shown). All chemosensory amphid cilia have one (ASE, ASG, ASH, ASI, ASJ, ASK) or two (ADF, ADL) slim, finger-like cylinders while the amphid wing cilia (AWA, AWB, AWC) have fan-like shapes[80]. (Unmodified figure from WormAtlas.[79])

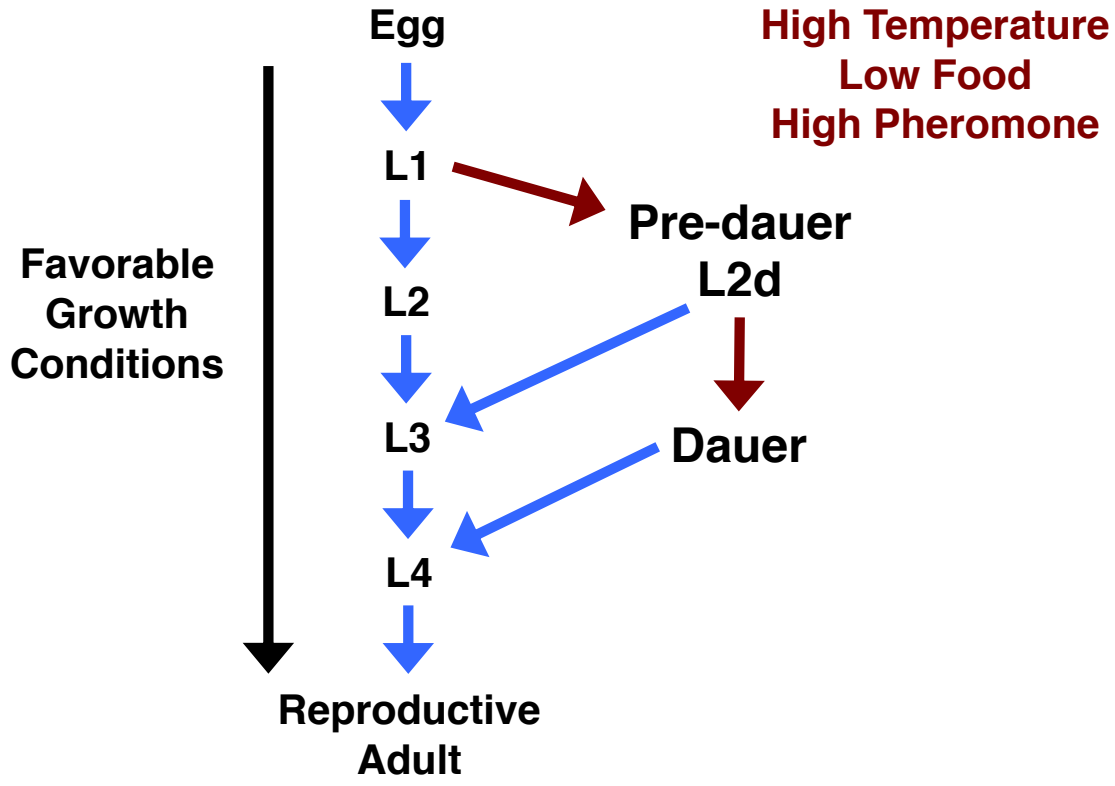

Figure 5: Life cycle of *C. elegans*. Blue arrows indicate trajectory under favorable conditions. Red arrows indicate trajectory under unfavorable conditions.

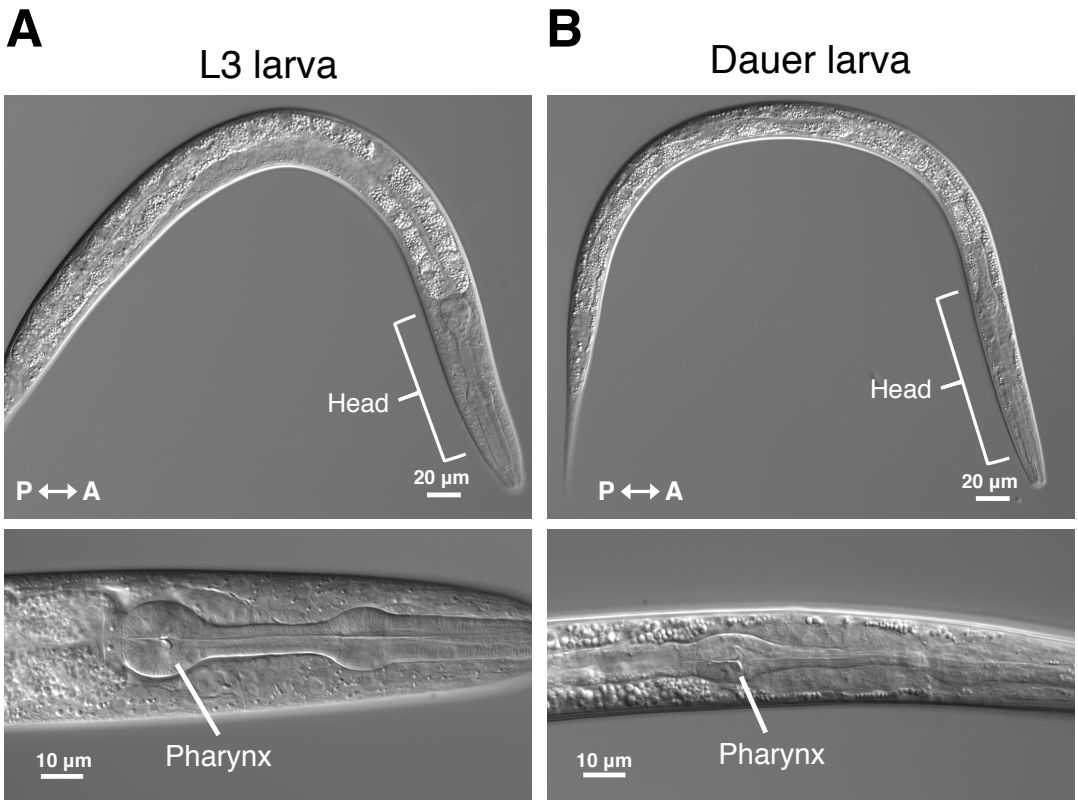

Figure 6: Dauer larva versus L3 larva morphology.

(A) Top – Whole-animal view of a L3 stage larva on the reproductive trajectory. The developing gonad is elongated and has many germ cell nuclei. Bottom – L3 larva head. Nerve ganglia can be seen surrounding pharynx.

(B) Top - Whole-animal view of a dauer stage larva on the diapause trajectory. Gonad development is arrested. Body is radially constricted and lipid droplets in intestine are enlarged. Bottom – Dauer larva head. Pharynx and nerve ganglia are radially constricted. Thickened cuticle is visible.

1.5 References

1. Brenner, S. The genetics of Caenorhabditis elegans. *Genetics* (1974). doi:10.1093/genetics/77.1.71
2. Sulston, J. E., Albertson, D. G. & Thomson, J. N. The Caenorhabditis elegans male: Postembryonic development of nongonadal structures. *Dev. Biol.* (1980). doi:10.1016/0012-1606(80)90352-8
3. White, J. G., Southgate, E., Thomson, J. N. & Brenner, S. The structure of the nervous system of the nematode Caenorhabditis elegans. *Philos. Trans. R. Soc. Lond. B. Biol. Sci.* **314**, 1–340 (1986).
4. Ward, A., Liu, J., Feng, Z. & Xu, X. Z. S. Light-sensitive neurons and channels mediate phototaxis in C. elegans. *Nat. Neurosci.* (2008). doi:10.1038/nn.2155
5. Chalfie, M. *et al.* The neural circuit for touch sensitivity in Caenorhabditis elegans. *J. Neurosci.* (1985). doi:10.1523/jneurosci.05-04-00956.1985
6. Mori, I. & Ohshima, Y. Neural regulation of thermotaxis in Caenorhabditis elegans. *Nature* (1995). doi:10.1038/376344a0
7. Hobert, O. The neuronal genome of Caenorhabditis elegans. *WormBook : the online review of C. elegans biology* (2013). doi:10.1895/wormbook.1.161.1
8. Janssen, T., Lindemans, M., Meelkop, E., Temmerman, L. & Schoofs, L. Coevolution of neuropeptidergic signaling systems: From worm to man. in *Annals of the New York Academy of Sciences* (2010). doi:10.1111/j.1749-6632.2010.05506.x
9. Wenick, A. S. & Hobert, O. Genomic cis-regulatory architecture and trans-acting regulators of a single interneuron-specific gene battery in C. elegans. *Dev. Cell* (2004). doi:10.1016/j.devcel.2004.05.004
10. Keating, C. D. *et al.* Whole-Genome Analysis of 60 G Protein-Coupled Receptors in Caenorhabditis elegans by Gene Knockout with RNAi. *Curr. Biol.* (2003). doi:10.1016/j.cub.2003.09.003
11. Pereira, L. *et al.* A cellular and regulatory map of the cholinergic nervous system of C. Elegans. *Elife* (2015). doi:10.7554/eLife.12432
12. Serrano-Saiz, E. *et al.* XModular control of glutamatergic neuronal identity in C. elegans by distinct homeodomain proteins. *Cell* (2013). doi:10.1016/j.cell.2013.09.052
13. Mclntire, S. L., Jorgensen, E., Kaplan, J. & Horvitz, H. R. The GABAergic nervous system of Caenorhabditis elegans. *Nature* (1993). doi:10.1038/364337a0
14. Yates, D. M., Portillo, V. & Wolstenholme, A. J. The avermectin receptors of Haemonchus contortus and Caenorhabditis elegans. in *International Journal for Parasitology* (2003). doi:10.1016/S0020-7519(03)00172-3
15. Putrenko, I., Zakikhani, M. & Dent, J. A. A family of acetylcholine-gated chloride channel subunits in Caenorhabditis elegans. *J. Biol. Chem.* (2005). doi:10.1074/jbc.M412644200
16. Brakefield, P. M., Pijpe, J. & Zwaan, B. J. Developmental plasticity and acclimation both contribute to adaptive responses to alternating seasons of plenty and of stress in Bicyclus butterflies. *J. Biosci.* (2007). doi:10.1007/s12038-007-0046-8
17. Brakefield, P. M., Kesbeke, F. & Koch, P. B. The regulation of phenotypic plasticity

of eyespots in the butterfly Bicyclus anynana. *Am. Nat.* (1998). doi:10.1086/286213
18. Petrusek, A., Tollrian, R., Schwenk, K., Haas, A. & Laforsch, C. A 'crown of thorns' is an inducible defense that protects Daphnia against an ancient predator. *Proc. Natl. Acad. Sci. U. S. A.* (2009). doi:10.1073/pnas.0808075106
19. Bateson, P. *et al.* Developmental plasticity and human health. *Nature* (2004). doi:10.1038/nature02725
20. Podrabsky, J. E. & Hand, S. C. The bioenergetics of embryonic diapause in an annual killifish, Austrofundulus limnaeus. *J. Exp. Biol.* (1999).
21. Wourms, J. P. Pre-embryonic and embryonic diapause of variable duration in the eggs of annual fishes. *J. Exp. Zool.* (1972).
22. Popiel, I., Grove, D. L. & Friedman, M. J. Infective juvenile formation in the insect parasitic nematode Steinernema feltiae. *Parasitology* (1989). doi:10.1017/S0031182000061047
23. Ghalambor, C. K., McKay, J. K., Carroll, S. P. & Reznick, D. N. Adaptive versus non-adaptive phenotypic plasticity and the potential for contemporary adaptation in new environments. *Funct. Ecol.* (2007). doi:10.1111/j.1365-2435.2007.01283.x
24. Golden, J. W. & Riddle, D. L. A pheromone influences larval development in the nematode Caenorhabditis elegans. *Science (80-.).* (1982). doi:10.1126/science.6896933
25. Byerly, L., Scherer, S. & Russell, R. L. The life cycle of the nematode Caenorhabditis elegans. *Dev. Biol.* (1976). doi:10.1016/0012-1606(76)90120-2
26. Cassada, R. C. & Russell, R. L. The dauerlarva, a post-embryonic developmental variant of the nematode Caenorhabditis elegans. *Dev. Biol.* **46**, 326–342 (1975).
27. Golden, J. W. & Riddle, D. L. The Caenorhabditis elegans dauer larva: Developmental effects of pheromone, food, and temperature. *Dev. Biol.* (1984). doi:10.1016/0012-1606(84)90201-X
28. Lee, S. S. & Schroeder, F. C. Steroids as central regulators of organismal development and lifespan. *PLoS Biol.* (2012). doi:10.1371/journal.pbio.1001307
29. Albert, P. S. & Riddle, D. L. Developmental alterations in sensory neuroanatomy of the Caenorhabditis elegans dauer larva. *J. Comp. Neurol.* (1983). doi:10.1002/cne.902190407
30. Hellerer, T. *et al.* Monitoring of lipid storage in Caenorhabditis elegans using coherent anti-Stokes Raman scattering (CARS) microscopy. *Proc. Natl. Acad. Sci. U. S. A.* (2007). doi:10.1073/pnas.0703594104
31. Narbonne, P. & Roy, R. Inhibition of germline proliferation during C. elegans dauer development requires PTEN, LKB1 and AMPK signalling. *Development* (2006). doi:10.1242/dev.02232
32. Schroeder, N. E. *et al.* Dauer-specific dendrite arborization in C. elegans is regulated by KPC-1/furin. *Curr. Biol.* (2013). doi:10.1016/j.cub.2013.06.058
33. Gerstein, M. B. *et al.* Integrative Analysis of the Caenorhabditis elegans Genome by the modENCODE Project. *Science (80-.)*. **330**, 1775–1787 (2010).
34. Lee, J. S. *et al.* FMRFamide-like peptides expand the behavioral repertoire of a densely connected nervous system. *Proc. Natl. Acad. Sci. U. S. A.* (2017). doi:10.1073/pnas.1710374114
35. Vidal, B. *et al.* An atlas of Caenorhabditis elegans chemoreceptor expression. *PLoS*

Biol. (2018). doi:10.1371/journal.pbio.2004218

36. Bhattacharya, A., Aghayeva, U., Berghoff, E. G. & Hobert, O. Plasticity of the Electrical Connectome of C. elegans. *Cell* (2019). doi:10.1016/j.cell.2018.12.024
37. Lee, H. *et al.* Nictation, a dispersal behavior of the nematode Caenorhabditis elegans, is regulated by IL2 neurons. *Nat. Neurosci.* (2012). doi:10.1038/nn.2975
38. Hallem, E. A. *et al.* A sensory code for host seeking in parasitic nematodes. *Curr. Biol.* (2011). doi:10.1016/j.cub.2011.01.048
39. Pungaliya, C. *et al.* A shortcut to identifying small molecule signals that regulate behavior and development in Caenorhabditis elegans. *Proc. Natl. Acad. Sci. U. S. A.* (2009). doi:10.1073/pnas.0811918106
40. Butcher, R. A., Fujita, M., Schroeder, F. C. & Clardy, J. Small-molecule pheromones that control dauer development in Caenorhabditis elegans. *Nat. Chem. Biol.* **3**, 420–422 (2007).
41. Jeong, P. Y. *et al.* Chemical structure and biological activity of the Caenorhabditis elegans dauer-inducing pheromone. *Nature* (2005). doi:10.1038/nature03201
42. Srinivasan, J. *et al.* A blend of small molecules regulates both mating and development in Caenorhabditis elegans. *Nature* **454**, 1115–1118 (2008).
43. Von Reuss, S. H. *et al.* Comparative metabolomics reveals biogenesis of ascarosides, a modular library of small-molecule signals in C. elegans. *J. Am. Chem. Soc.* (2012). doi:10.1021/ja210202y
44. Gallo, M. & Riddle, D. L. Effects of a Caenorhabditis elegans dauer pheromone ascaroside on physiology and signal transduction pathways. *J. Chem. Ecol.* (2009). doi:10.1007/s10886-009-9599-3
45. Srinivasan, J. *et al.* A modular library of small molecule signals regulates social behaviors in Caenorhabditis elegans. *PLoS Biol.* (2012). doi:10.1371/journal.pbio.1001237
46. Butcher, R. A., Ragains, J. R., Kim, E. & Clardy, J. A potent dauer pheromone component in Caenorhabditis elegans that acts synergistically with other components. *Proc. Natl. Acad. Sci. U. S. A.* (2008). doi:10.1073/pnas.0806676105
47. Park, D. *et al.* Interaction of structure-specific and promiscuous G-protein-coupled receptors mediates small-molecule signaling in Caenorhabditis elegans. *Proc. Natl. Acad. Sci. U. S. A.* (2012). doi:10.1073/pnas.1202216109
48. McGrath, P. T. *et al.* Parallel evolution of domesticated Caenorhabditis species targets pheromone receptor genes. *Nature* (2011). doi:10.1038/nature10378
49. Kim, K. *et al.* Two Chemoreceptors Mediate Developmental Effects of Dauer Pheromone in C. elegans. *Science (80-.).* **326**, 994–998 (2009).
50. Park, D. *et al.* Interaction of structure-specific and promiscuous G-protein-coupled receptors mediates small-molecule signaling in Caenorhabditis elegans. *Proc. Natl. Acad. Sci.* **109**, 9917–9922 (2012).
51. Robertson, H. M. & Thomas, J. H. The putative chemoreceptor families of C. elegans. *WormBook : the online review of C. elegans biology* (2006). doi:10.1895/wormbook.1.66.1
52. Choe, A. *et al.* Ascaroside signaling is widely conserved among nematodes. *Curr. Biol.* **22**, 772–780 (2012).
53. Bento, G., Ogawa, A. & Sommer, R. J. Co-option of the hormone-signalling module

dafachronic acid-DAF-12 in nematode evolution. *Nature* (2010). doi:10.1038/nature09164

54. Ren, P. *et al.* Control of C. elegans larval development by neuronal expression of a TGF-β homolog. *Science (80-.).* (1996). doi:10.1126/science.274.5291.1389
55. Schackwitz, W. S., Inoue, T. & Thomas, J. H. Chemosensory neurons function in parallel to mediate a pheromone response in C. elegans. *Neuron* **17**, 719–728 (1996).
56. Georgi, L. L., Albert, P. S. & Riddle, D. L. daf-1, a C. elegans gene controlling dauer larva development, encodes a novel receptor protein kinase. *Cell* (1990). doi:10.1016/0092-8674(90)90475-T
57. Estevez, M. *et al.* The daf-4 gene encodes a bone morphogenetic protein receptor controlling C. elegans dauer larva development. *Nature* (1993). doi:10.1038/365644a0
58. Patterson, G. I., Koweek, A., Wong, A., Liu, Y. & Ruvkun, G. The DAF-3 Smad protein antagonizes TGF-β-related receptor signaling in the Caenorhabditis elegans dauer pathway. *Genes Dev.* (1997). doi:10.1101/gad.11.20.2679
59. Inoue, T. & Thomas, J. H. Targets of TGF-β signaling in caenorhabditis elegans dauer formation. *Dev. Biol.* (2000). doi:10.1006/dbio.1999.9545
60. da Graca, L. S. *et al.* DAF-5 is a SKi oncoprotein homolog that functions in a neuronal TGFβ pathway to regulate C. elegans dauer development. *Development* (2004). doi:10.1242/dev.00922
61. Tewari, M. *et al.* Systematic interactome mapping and genetic perturbation analysis of a C. elegans TGF-β signaling network. *Mol. Cell* (2004). doi:10.1016/S1097-2765(04)00033-4
62. Pierce, S. B. *et al.* Regulation of DAF-2 receptor signaling by human insulin and ins-1, a member of the unusually large and diverse C. elegans insulin gene family. *Genes Dev.* (2001). doi:10.1101/gad.867301
63. Li, W., Kennedy, S. G. & Ruvkun, G. daf-28 encodes a C. elegans insulin superfamily member that is regulated by environmental cues and acts in the DAF-2 signaling pathway. *Genes Dev.* (2003). doi:10.1101/gad.1066503
64. Murphy, C. T. *et al.* Genes that act downstream of DAF-16 to influence the lifespan of Caenorhabditis elegans. *Nature* (2003). doi:10.1038/nature01789
65. Kimura, K. D., Tissenbaum, H. A., Liu, Y. & Ruvkun, G. Daf-2, an insulin receptor-like gene that regulates longevity and diapause in Caenorhabditis elegans. *Science (80-.).* (1997). doi:10.1126/science.277.5328.942
66. Gottlieb, S. & Ruvkun, G. daf-2, daf-16 and daf-23: Genetically interacting genes controlling dauer formation in Caenorhabditis elegans. *Genetics* (1994). doi:10.1093/genetics/137.1.107
67. Kenyon, C., Chang, J., Gensch, E., Rudner, A. & Tabtiang, R. A C. elegans mutant that lives twice as long as wild type. *Nature* (1993). doi:10.1038/366461a0
68. Morris, J. Z., Tissenbaum, H. A. & Ruvkun, G. A phosphatidylinositol-3-OH kinase family member regulating longevity and diapause in Caenorhabditis elegans. *Nature* (1996). doi:10.1038/382536a0
69. Paradis, S., Ailion, M., Toker, A., Thomas, J. H. & Ruvkun, G. A PDK1 homolog is necessary and sufficient to transduce AGE-1 PI3 kinase signals that regulate diapause in Caenorhabditis elegans. *Genes Dev.* (1999). doi:10.1101/gad.13.11.1438

70. Paradis, S. & Ruvkun, G. Caenorhabditis elegans Akt/PKB transduces insulin receptor-like signals from age-1 PI3 kinase to the DAF-16 transcription factor. *Genes Dev.* (1998). doi:10.1101/gad.12.16.2488
71. Hertweck, M., Göbel, C. & Baumeister, R. C. elegans SGK-1 is the critical component in the Akt/PKB kinase complex to control stress response and life span. *Dev. Cell* (2004). doi:10.1016/S1534-5807(04)00095-4
72. Henderson, S. T. & Johnson, T. E. daf-16 integrates developmental and environmental inputs to mediate aging in the nematode Caenorhabditis elegans. *Curr. Biol.* (2001). doi:10.1016/S0960-9822(01)00594-2
73. Lin, K., Hsin, H., Libina, N. & Kenyon, C. Regulation of the Caenorhabditis elegans longevity protein DAF-16 by insulin/IGF-1 and germline signaling. *Nat. Genet.* (2001). doi:10.1038/88850
74. Lee, R. Y. N., Hench, J. & Ruvkun, G. Regulation of C. elegans DAF-16 and its human ortholog FKHRL1 by the daf-2 insulin-like signaling pathway. *Curr. Biol.* (2001). doi:10.1016/S0960-9822(01)00595-4
75. Perens, E. A. & Shaham, S. C. elegans daf-6 encodes a patched-related protein required for lumen formation. *Dev. Cell* (2005). doi:10.1016/j.devcel.2005.03.009
76. Bell, L. R., Stone, S., Yochem, J., Shaw, J. E. & Herman, R. K. The molecular identities of the caenorhabditis elegans intraflagellar transport genes dyf-6, daf-10 and osm-1. *Genetics* (2006). doi:10.1534/genetics.106.056721
77. Perkins, L. A., Hedgecock, E. M., Thomson, J. N. & Culotti, J. G. Mutant sensory cilia in the nematode Caenorhabditis elegans. *Dev. Biol.* (1986). doi:10.1016/0012-1606(86)90314-3
78. Bargmann, C. I. & Horvitz, H. R. Control of larval development by chemosensory neurons in Caenorhabditis elegans. *Science* **251**, 1243–6 (1991).
79. Altun, Z. F. *et al.* WormAtlas and WormImage: The Websites and the Book. *International Worm Meeting* (2007).
80. Ward, S., Thomson, N., White, J. G. & Brenner, S. Electron microscopical reconstruction of the anterior sensory anatomy of the nematode caenorhabditis elegans. *J. Comp. Neurol.* (1975). doi:10.1002/cne.901600305

CHAPTER 2: Interneuron control of developmental plasticity

2.1 Abstract

To maximize fitness, animals integrate various external stimuli to sculpt their physiological and behavioral responses throughout development. Under adverse environmental conditions, *C. elegans* larvae can choose to enter an alternate stress-resistant diapause state during which metabolism and reproductive physiology are arrested. *C. elegans* constitutively secretes dauer larvae-inducing pheromone, which serves as a proxy for high conspecific density. This information about local competition is integrated with other inputs to assess the environment's suitability for future reproductive growth. Although the roles of individual chemosensory neurons are well studied, much less is known about how these inputs are integrated and whether other neuron classes participate in this developmental paradigm. Here, we delineate how a pair of first layer amphid interneurons integrates conspecific cues and propagates this information via neuropeptidergic pathways to influence larval developmental fate. We show that the AIA interneurons secrete the neuropeptide FLP-2 to promote reproductive development and that AIA activity is inhibited by pheromone. We also show that FLP-2's growth promoting effects are inhibited by upstream glutamatergic signaling via the metabotropic glutamate receptor MGL-1. We further identify the broadly-expressed neuropeptide receptor NPR-30 downstream of FLP-2 and implicate AIA's major postsynaptic partner, the AIB interneurons, in this decision-making circuit. These results expand our knowledge of the neural and genetic players in the complex developmental fate determination circuitry that dictates an organism's life history.

2.2 Introduction

Natural environments are highly dynamic and this complexity challenges animals to accurately integrate external cues to shape their responses. Phenotypic plasticity is the ability of a genotype to produce more than one phenotype depending on the external environment experienced. This adaptive strategy enables organisms to remodel their morphology, physiology, and behavior to better suit the predicted future environment and ultimately enhance their ecological success[1]. Unlike behavioral plasticity, developmental plasticity often results in longer-lasting changes such as switches in developmental trajectories that irreversibly alter the adult phenotype or, in some cases, induce reversible larval arrest[2]. Examples of developmental plasticity include thermal regulation of *Drosophila melanogaster* body size[3–5], accelerated reproductive senescence in red deer that have experienced early-life resource scarcity[6,7], and protective helmet development in *Daphnia* in response to predator presence[8,9]. Despite the pervasiveness of this strategy in nature, little is known about the neural and molecular mechanisms that transduce external inputs into effector pathways that orchestrate the alternative developmental phenotype. While the recent advent of transcriptomics has made possible the generation of large state-specific gene expression datasets, the lack of genetic accessibility in non-model organisms often precludes defining causal relationships between changes in gene product quantity and the observed phenotypes. Furthermore, the complexity of mammalian and fly models complicates a comprehensive study of multi-tissue modulatory pathways downstream of neural signaling. Here, we leverage the well-defined genetics and nervous system of *C. elegans* to dissect the sensory integration pathways controlling developmental plasticity.

Under adverse environmental conditions, *C. elegans* L1 larvae can enter an alternate developmental trajectory where they first form preparatory pre-dauer L2d larvae before fully committing to entering the stress-resistant dauer stage[10]. The transition into diapause is accompanied by several adaptations that enable the larva to endure and survive deleterious conditions. Dauer larvae have thickened cuticles, enlarged lipid droplet stores, arrested gonad development, and are radially constricted compared to their reproductive L3 stage counterparts[11]. Synaptic rewiring of the nervous system and neuropeptide expression changes also give rise to dauer stage-specific behaviors such as nictation, carbon dioxide

attraction, and cessation of pharyngeal pumping[12–15]. Once in the dauer stage, larvae can survive for up to 8 months without food and can revert to the reproductive trajectory at any point during this period should external conditions improve[11,16]. The *C. elegans* decision to enter diapause is informed by multimodal sensory cues. Coincident detection of high pheromone concentrations, high temperatures, and low food availability by the larval sensory apparatus triggers diapause entry[10,17]. *C. elegans* constitutively secretes a mixture of dideoxy sugar ascarylose derivatives that comprise dauer larvae-inducing pheromone, and is used as a measure of local conspecific competition for limited resources[18–20]. These small-molecule ascarosides bind to seven transmembrane domain receptors located in chemosensory neuron cilia to trigger intracellular signaling cascades that alter neuronal activity[21,22].

The majority of previous literature on the neural control of diapause entry has focused on the contributions of sensory neurons. Systematic laser and genetic ablations of sensory neuron classes have revealed that six of the eleven amphid chemosensory neuron classes mediate diapause entry to varying extents in a context-dependent manner[22–24]. For example, ablation of the ASK sensory neurons under pheromone dauer-inducing conditions results in a more dramatic reduction of dauers formed compared to similar experiments performed in the absence of pheromone[22]. Sensory neurons are also the main sources of neuroendocrine ligands like DAF-7/TGF-ß (ASI neurons) and neuromodulators like serotonin (ADF neurons) that promote reproductive growth by acting on multiple tissues[23,25]. It is thus plausible that sensory layer circuits account for all integrative computations of multimodal stimuli, which then bypasses interneuron processing by directly executing modulatory pathways to influence developmental fate. In contrast, *C. elegans* neurobehavioral studies generally involve a hierarchical organization of information flow from the sensory layer to interneurons and finally to effector motor neurons[26]. The first layer amphid interneurons AIA, AIB, AIY, and AIZ are so termed because they receive extensive synaptic inputs from sensory neurons residing within the amphid organ in the head[27]. They then relay this information to the second layer amphid interneurons RIA, RIB, and RIM, which are presynaptic to command interneurons[27].

Here, we examine whether a similar circuit hierarchy is involved in mediating *C. elegans* developmental plasticity. To model the stressful dauer-inducing conditions

encountered by *C. elegans* in the wild, we incubate developing larvae at elevated temperatures while continuously exposing them to crude pheromone extract and a low-quality, limited food source[12]. We find that the AIA interneurons contribute to developmental fate choice by integrating inhibitory inputs from pheromone-sensing neurons and propagating this information via neuropeptidergic pathways to affect broad downstream targets.

2.3 Results

AIA inhibition recapitulates the *flp-2* mutant dauer formation phenotype

To investigate if AIA activity affects larval developmental trajectory, we pharmacologically silenced AIA by expressing the *Drosophila* histamine-gated chloride channel HisCl1[28]. *C. elegans* does not synthesize or use histamine as an endogenous neurotransmitter[29]. We constitutively silenced AIA by growing AIA::HisCl1 animals on plates containing histamine and compared dauer formation with animals of the same genotype grown on control plates without histamine. We found that a significantly higher proportion of AIA-silenced animals entered diapause compared to the negative control, indicating that AIA promotes entry into the reproductive growth trajectory (Figure 1A).

As AIA inhibition increases dauer formation, AIA likely secretes a transmitter that promotes reproductive growth. Our lab has previously investigated the role of the FMRF-like peptide (*flp*) gene family in pheromone-induced dauer formation[12]. Among the *flp* genes screened, *flp-2*(*ok3351*) mutants formed more dauers compared to wild-type N2 (Figure 1B)[12]. The *ok3351* allele harbors a deletion that removes the first exon of both predicted *flp-2* transcripts and is thus likely to be a null mutation. *flp-2* expression has been reported in the AIA, RID, PVW, I5 and MC neurons[30]. A transcriptional reporter containing a truncated 2 kb fragment of upstream regulatory sequence 5' to the *flp-2* start codon fused to GFP was expressed strongly and consistently in a single pair of neurons in the head during the L1 stage (Figure 1C). We identified this pair of neurons as the AIA interneurons based on GFP expression colocalization with a nuclear-localized AIA-specific mCherry marker (Figure 1C)[31].

AIA-derived FLP-2 promotes larval entry into the reproductive growth trajectory

To determine if FLP-2 mediates AIA's reproductive growth-promoting role, we expressed *flp-2* cDNA in an AIA-dependent manner where it was sufficient to rescue the *flp-2* dauer formation phenotype (Figure 2A). Non-neuronal GFP expression was also visible in the intestine of the *flp-2* transcriptional GFP reporter but intestine-specific *flp-2* cDNA expression did not affect *flp-2* mutant dauer formation (Figure 2B). Since loss of FLP-2 signaling in the *flp-2*(*ok3351*) mutant leads to increased dauer formation, we wondered if an excess of the neuropeptide would have the opposite effect on larval development. Indeed, overexpression of *flp-2* in AIA resulted in reduced dauer formation compared to control animals (Figure 2C).

To confirm that FLP-2 peptides are secreted by AIA, we fused mCherry to the C-terminus of FLP-2 precursors in AIA. We detected both diffuse and vesicular mCherry expression in AIA's soma, which was visualized by soluble GFP (Figure 2D). In *C. elegans,* secreted proteins are released into the pseudocoelom and endocytosed by the coelomocyte scavenger cells[32]. The six coelomocyte scavenger cells are located in three pairs along the worm's body. During the L1 stage, we observed strong mCherry signal within GFP-expressing coelomocyte cells indicating FLP-2 peptide release and uptake (Figure 2E). Taken together, these results suggest that FLP-2 is an AIA-secreted signal that promotes reproductive development.

Pheromone activates ASK and ADL sensory neurons but inhibits downstream AIA interneurons

The AIA interneurons makes several chemical and electrical synaptic connections with all the amphid chemosensory neuron classes including ASK and ADL, which mediate adult responses to certain ascarosides (Figure 3A)[27]. Laser ablation and mutant analysis of ASK and ADL indicate that these neurons promote dauer formation under pheromone dauer-inducing conditions. To examine the relationship between sensory neuron activity and dauer formation, we silenced ASK and ADL by selective expression of *Drosophila HisCl1*. Silencing of either neuron class reduced dauer formation suggesting that ASK and ADL activity promotes diapause entry (Figure 3B, C). In adult animals, ASK intracellular calcium

levels are decreased by synthetic ascaroside cocktails that mediate adult aggregation and male-to-hermaphrodite attraction behaviors[33]. However, the crude pheromone extract used in this study is a mixture of ascaroside components in naturally-occurring proportions whose synergistic effects might elicit different responses. We sought to determine if and how crude pheromone extract modulates ASK and ADL responses by delivering a time-locked pheromone stimulus to restrained L4 stage animals expressing the genetically-encoded calcium sensor GCaMP6s in both neuron classes[34]. Pheromone delivery was accompanied by a fast, robust increase in intracellular calcium levels in ASK and ADL indicating that they detect and are activated by crude pheromone (Figure 3D, E). In addition, both paired partners in each class displayed symmetric responses to pheromone delivery.

AIA is depolarized when presented with synthetic ascaroside mixtures[33]. To probe if AIA responds similarly to crude pheromone extract, we delivered pheromone to physically restrained L4 animals expressing GCaMP6s in AIA only. We first recorded calcium influx changes in AIA's soma and could not detect any significant changes in AIA activity during pheromone delivery (Figure S1). As *C. elegans* interneurons exhibit compartmentalized calcium dynamics, we next measured GCaMP fluorescence changes in the AIA processes within the nerve ring where synaptic connections are densely concentrated[35]. In our microfluidics setup, AIA is frequently quiescent with only 20% of all animals assayed displaying spontaneous process activity before the onset of pheromone delivery. In this fraction of animals, pheromone delivery consistently suppressed spontaneous AIA process activity and removal of the pheromone stimulus was followed by a post-inhibitory activity rebound that was greater in amplitude compared to before pheromone delivery (Figure 3F). Thus, AIA activity is inhibited by crude pheromone extract. Furthermore, the opposite responses to pheromone of ASK and ADL compared to AIA implies that ASK and ADL make inhibitory connections to downstream AIA neurons.

The AWA olfactory sensory neurons sense and mediate *C. elegans* attraction to the odorant diacetyl, and is gap-junctioned to AIA (Figure 3A)[27,36]. Recently, an AND-gate logic model of AIA integrative function has been proposed where coincident inhibition of glutamatergic chemosensory neurons including ASK and activation of AWA by diacetyl leads to robust AIA activation in adult animals[37]. We wondered if exposure to diacetyl

concentrations that mediate behavioral responses might bias larval development towards the reproductive trajectory under our pheromone dauer-inducing assay conditions. However, we found that the diacetyl exposure throughout the assay duration did not affect dauer formation (Figure 3H). Higher diacetyl concentrations corresponded to stronger ASK inhibition, AWA activation, and AIA activation[37]. Thus, one explanation for our observation is that the diacetyl concentration used in our dauer formation assays was not high enough to disinhibit AIA.

FLP-2 signaling is inhibited by glutamatergic transmission via the metabotropic glutamate receptor MGL-1

Although glutamate is the major excitatory neurotransmitter in the vertebrate central nervous system, it can also have inhibitory effects depending on the type of glutamate receptors present in the postsynaptic membrane. ASK and ADL are glutamatergic neurons[38]. AIA expresses both the ionotropic glutamate-gated chloride channel GLC-3 and the G-protein coupled inhibitory metabotropic glutamate receptor MGL-1[39–43]. Thus, it is likely that inhibitory glutamatergic transmission from upstream ASK and ADL sensory neurons affects AIA-mediated FLP-2 signaling during developmental decision-making. To test this, we first determined if *glc-3* and *mgl-1* mutants had a dauer formation phenotype. We found that fewer *glc-3* and *mgl-1* mutants developed into dauers compared to control animals suggesting that inhibitory glutamatergic transmission via both receptors promotes pheromone-induced dauer formation (Figure 4A, B and Fig S2). If FLP-2 signaling is downstream of these inhibitory glutamatergic transmission pathways, we would expect the *flp-2* mutant's increase in dauer formation to mask the *glc-3* and/or *mgl-1* mutant's reduction in dauer formation phenotype during genetic epistasis analysis. *flp-2*; *glc-3* double mutants had an additive phenotype indicating that either GLC-3 does not mediate FLP-2 signaling (independent pathways) or only makes a minor contribution (Figure 4C). As *mgl-1* and *flp-2* reside on the same chromosome we generated a *flp-2*; *mgl-1* double mutant by CRISPR mutagenesis of the *mgl-1* locus in *flp-2* mutant background (see Methods). This *flp-2*; *mgl-1* double mutant phenocopied the *flp-2* single mutant's increased dauer formation phenotype (Figure 4D). Thus, although both *glc-3* and *mgl-1* have roles in pheromone-induced dauer formation,

MGL-1-mediated glutamatergic inhibition predominantly affects downstream FLP-2 signaling in the context of diapause entry.

AIB interneurons and their neuropeptide receptor NPR-9 promote diapause entry

We next focused on identifying downstream elements of the AIA-mediated developmental decision-making circuit. The AIB interneurons are AIA's main postsynaptic partners and the strong unidirectional synaptic connection from AIA to AIB is likely to be inhibitory based on behavioral studies (cite). Pharmacological silencing of AIB reduced dauer formation suggesting that the AIA and AIB first layer interneurons have antagonistic effects on larval developmental choice (Figure 5A). *npr-9* encodes a neuropeptide G-protein coupled receptor (GPCR) that is orthologous to human galanin receptor 2 GAL2 and is specifically expressed in the AIB neurons where it mediates adult foraging behavior[44]. *npr-9* mutants assayed for pheromone-induced dauer formation recapitulated the AIB-silenced decreased dauer formation phenotype suggesting that AIB's diapause entry-promoting role is mediated by NPR-9 signaling (Figure 5B). We wondered whether FLP-2 and NPR-9 mediate related or independent signaling pathways and turned to genetic epistasis analysis to probe this. As *npr-9* and *flp-2* are also on the same chromosome, we used a similar CRISPR-based strategy as with the *flp-2*; *mgl-1* strain to generate a *flp-2*; *npr-9* double mutant. The *flp-2*; *npr-9* double mutant phenocopied the *flp-2* single mutant's increased dauer formation phenotype indicating that flp-2 is downstream of *npr-9* in the same genetic pathway that influences developmental fate (Figure 5C).

The broadly-expressed neuropeptide receptor NPR-30 mediates FLP-2 signaling

In vitro studies indicate that peptides encoded by the *flp-2* precursor bind to the neuropeptide GPCR FRPR-18 in a heterologous mammalian cell expression system[45]. However, *frpr-18* mutants had a reduced dauer formation phenotype (Figure 6A). Furthermore, *flp-2*; *frpr-18* double mutants exhibit an additive phenotype that is significantly different from both the *flp-2* and *frpr-18* single mutant controls (Figure 6B). These results suggest that *flp-2* and *frpr-18* do not act in the same genetic pathway in the context of dauer formation.

We continued our search for potential downstream receptor targets of FLP-2 by conducting a preliminary dauer formation screen of all available neuropeptide GPCR mutants in our strain collection (data not shown). We identified *npr-30* mutants as having an increased dauer formation phenotype and show that the *npr-30* mutation completely suppressed the *flp-2* overexpression reduced dauer formation phenotype (Figure 6C, D). In addition, the *flp-2*; *npr-30* double mutant dauer formation phenotype was not significantly different from either the *flp-2* or *npr-30* single mutant phenotypes (Figure 6E). Taken together, these data suggest that *npr-30* is downstream of *flp-2* in the same pathway mediating the diapause entry decision.

To determine where *npr-30* is expressed, we generated a *npr-30* translational reporter containing an 8.5 kb *npr-30* genomic fragment linked to GFP by an SL2-spliced intercistronic region. During the L1 stage, GFP was broadly expressed in the nervous system as well as in the intestine (Figure 6F). In the nervous system, we observed expression in sensory neurons, interneurons, and motor neurons suggesting that FLP-2 signaling exerts global modulatory effects via NPR-30 (Figure 6F). Besides acting on other targets, FLP-2 might also mediate a positive AIA autoregulatory feedback loop to drive and sustain commitment to reproductive growth under favorable conditions. However, our *npr-30* translational GFP reporter did not colocalize with an AIA-specific mCherry marker indicating that this motif is unlikely (Figure 6G).

INS-1 and FLP-2 have antagonistic roles in developmental decision-making

In *C. elegans*, individual neuron classes typically express a constellation of neuropeptide precursor genes[46]. In addition to *flp-2*, AIA also co-expresses the insulin-related neuropeptide-encoding *ins-1*[47]. AIA-specific INS-1 release mediates normal turning behavior during odor-evoked local search[48]. Therefore we decided to investigate if AIA-derived INS-1 might play a role in pheromone-induced dauer formation. Unlike *flp-2* mutants, *ins-1* mutants exhibited a decreased dauer formation phenotype (Figure 7A). Furthermore, the *flp-2*; *ins-1* double mutant displayed an additive phenotype that was significantly different from both the *flp-2* and *ins-1* single mutant phenotypes suggesting that these neuropeptides act in independent processes (Figure 7B). Can a single neuron class

simultaneously mediate antagonistic neuropeptidergic pathways in the same paradigm? To resolve this apparent paradox, we expressed *ins-1* in an AIA-specific manner in *ins-1* mutant background where it did not affect the mutant's dauer formation phenotype (Figure 7C). As *ins-1* is expressed in many neurons besides AIA and overexpression of *ins-1* under the control of *ins-1* regulatory sequences enhances dauer formation, it is likely that INS-1 secretion by other neurons antagonizes FLP-2 signaling[47,49].

2.4 Discussion

Here, we show that a pair of interneurons controls the switch between different larval developmental trajectories depending on prevailing environmental conditions. Under favorable conditions, AIA is active and secretes the neuropeptide FLP-2 which promotes reproductive growth (Figure 8A). FLP-2 signaling is mediated by the neuropeptide receptor NPR-30 which is broadly expressed in the neurons and the intestine (Figure 8A). As conspecific population density and competition for limited resources increases, the concentration of secreted pheromone in the local area also increases. This pheromone cue activates the ASK and ADL sensory neurons which in turn inhibits the downstream AIA interneurons (Figure 8B). FLP-2 signaling is inhibited by glutamatergic transmission mediated by the inhibitory metabotropic glutamate receptor MGL-1 resulting in more larvae choosing to enter diapause (Figure 8B). We also find that AIA's main post-synaptic partner, the AIB interneurons, promotes diapause entry hinting at an inhibitory connection between both neuron classes (Figure 8C). Furthermore, the AIB-specific galanin-like neuropeptide receptor NPR-9 also promotes diapause entry. Finally we show that AIA-independent INS-1 signaling antagonizes FLP-2's growth-promoting effects. Thus, we have systematically dissected how sensory cues are transduced by an integrative interneuron into neuropeptidergic signals that shape larval developmental decision-making.

Diapause entry can be maladaptive if an incorrect assessment of environmental conditions is made since dauer larvae can take 16-20 hours to fully re-enter the trajectory leading to reproductive adulthood[11]. The metabolic costs of physiological remodeling coupled with the delay in nutritional intake (dauers are non-feeding) can negatively impact future reproductive success. Thus, we would expect such an important calculation to be under

the control of complex, distributed regulatory networks as opposed to relying on a more efficient sparse-coding scheme that is less robust when challenged with noisy inputs from nature. In this study, we have expanded the known neural circuit regulating diapause entry by implicating two new first layer amphid interneurons AIA and AIB in this paradigm. There is likely to be more neuron classes involved in this circuit, especially other interneurons that lie at the confluence of multiple upstream sensory modalities and have neuromodulatory capabilities. A key motivation behind this study was to determine if information flow during developmental decision-making followed the same generalized hierarchical structure as behavior. Based on our findings, the interneuron layer does contribute to the diapause entry decision in an integrative capacity although it would be interesting to see whether interneuron-derived signals eventually feed back to the sensory layer which then executes terminal effector pathways that 'locks in' larval fate.

The results of our microfluidics experiments show that acute inhibition of AIA by pheromone is followed by a sharp increase in calcium influx immediately after pheromone delivery is terminated. This observed post-inhibitory increase in AIA activity appears to contradict our functional dauer formation assays which indicate that pheromone dauer-inducing environments inhibit AIA-derived FLP-2 signaling. However, the AIA response to acute pheromone presentation is likely to be mediated by the fast ionotropic GLC-3 receptor channel. Based on our *flp-2* epistasis analysis results, FLP-2 signaling is largely mediated by the slower-acting metabotropic MGL-1 receptor. In addition, larvae are exposed to lower pheromone concentrations over a much longer timescale during dauer formation assays compared to the microfluidics setup. Thus, post-inhibitory activity rebounds driven by acute neuronal inhibition might not be occurring during the actual diapause entry decision-making process. While acute pheromone delivery is useful for identifying the valence of a neuron's response to the stimulus, it is insufficient to accurately determine larval neuronal dynamics over developmentally-relevant timescales. Recent advances in long-term functional imaging of neurons in larvae cultured in agarose microchambers will be useful for this application[50,51].

The MGL-1 receptor mediates foraging behavior and reproductive plasticity in adult *C. elegans*, and is expressed in just four interneuron classes AIA, RMD, AIY, and NSM[43,52]. Here, we show that MGL-1 plays a critical role in establishing an alternative larval phenotype

over developmentally-relevant timescales by inhibiting growth-promoting FLP-2 neuropeptide signaling. MGL-1 is an ortholog of the vertebrate Group II glutamate metabotropic receptors mGluR2 and mGluR3, which are expressed in the hypothalamus and pituitary gland[53]. When activated by glutamate binding, the Group II mGluRs inhibit cAMP production as a result of their negative coupling to adenylate cyclase resulting in inhibition of the receptor-expressing neuron[54]. In vertebrate nervous systems, the hypothalamus receives inputs from multiple sensory modalities and integrates this wide range of information to drive appropriate behavioral and physiological responses[55]. In particular, the hypothalamic-pituitary axis of transmission mediates many aspects of growth, development, and the response to stressful stimuli through neuroendocrine regulation[55]. In these brain regions, glutamatergic neurotransmission via group II mGluRs inhibits the release of neuroendocrine factors[53,56]. Similarly in *C. elegans*, we find that the AIA interneurons act as an integrative hub that translates inhibitory glutamatergic neurotransmission into downregulation of neuropeptidergic signaling that ultimately impacts energy metabolism, reproductive physiology, and organismal morphology.

2.5 Figures

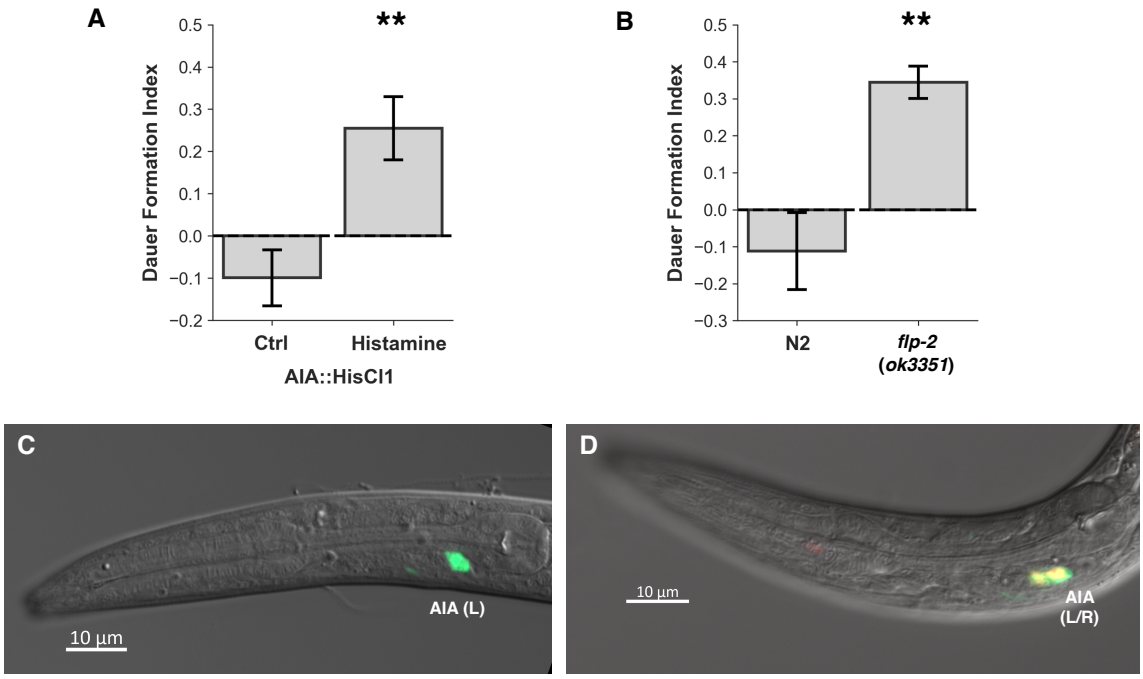

Figure 1. AIA inhibition recapitulates the *flp-2* mutant dauer formation phenotype.

(A) Dauer formation assays for AIA::*HisCl1* animals grown on plates with and without histamine. N=9 population assays. Data represented as mean ± SEM, student's t-test equal variance, **p<0.01.

(B) Dauer formation assays for *flp-2* mutants. N=5-6 population assays. Data represented as mean ± SEM, student's t-test equal variance, **p<0.01.

(C) P*flp-2*::*GFP* expression in an L1 stage larva.

(D) P*flp-2*::*GFP* colocalization with P*gcy-28*.d::*mCherry-H2B* in an L1 stage larva.

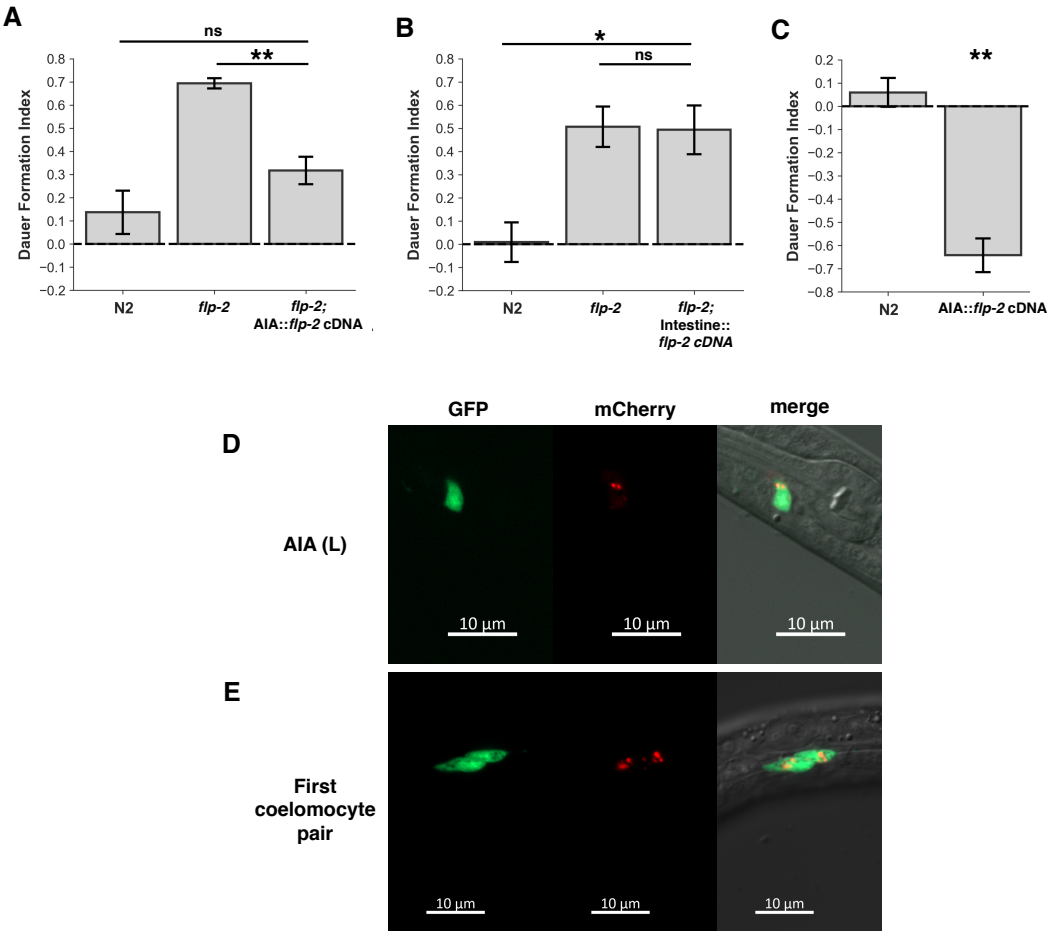

Figure 2. AIA-derived FLP-2 promotes larval entry into the reproductive growth trajectory.

(A) Dauer formation assays for AIA-specific *flp-2* cDNA expression in *flp-2* mutants. N=5 population assays. Data represented as mean ± SEM, ANOVA followed by Dunnett's compared to *flp-2*; AIA::*flp-2* cDNA, ns=no significance, **p<0.01.

(B) Dauer formation assays for intestine-specific *flp-2* cDNA expression in *flp-2* mutants. N=3-4 population assays. Data represented as mean ± SEM, ANOVA followed by Dunnett's compared to flp-2; Intestine::*flp-2* cDNA, ns=no significance, *p<0.05.

(C) Dauer formation assays for AIA-specific *flp-2* cDNA overexpression. N=3 population assays. Data represented as mean ± SEM, student's t-test equal variance, **p<0.01.

(D) AIA::*flp-2* cDNA::*mCherry* colocalization with AIA::*GFP* in an L1 stage larva.

(E) mCherry colocalization with first pair of coelomocytes visualized with P*ofm-1*::*GFP* in an L1 stage larva.

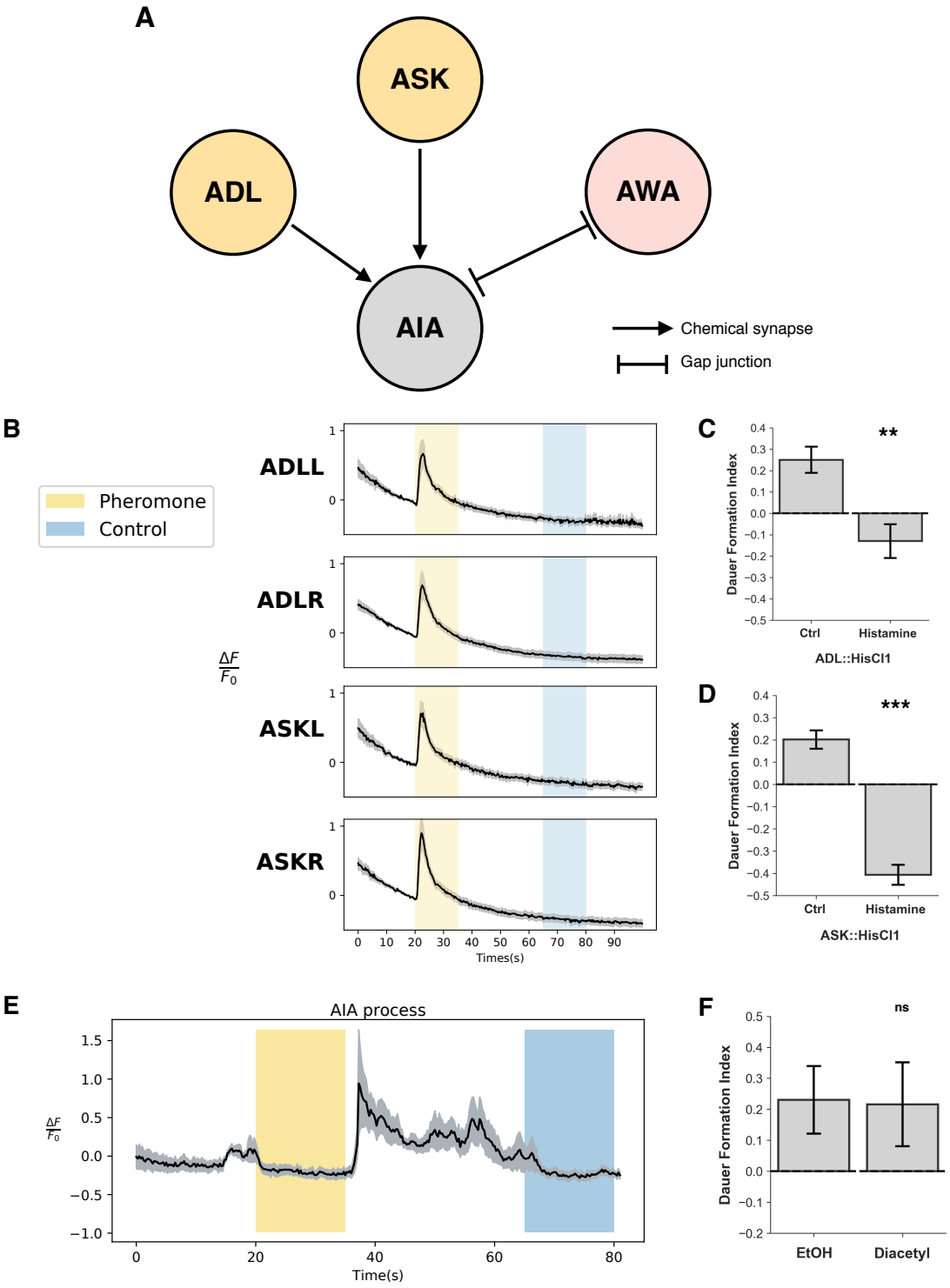
A
ASK
ADL
AWA
AIA
Chemical synapse
Gap junction
B
Pheromone
Control
ADLL
ADLR
ASKL
ASKR
ΔF/F0
Times(s)
C
**
Dauer Formation Index
Ctrl
Histamine
ADL::HisCl1
D
***
ASK::HisCl1
E
AIA process
Time(s)
F
ns
EtOH
Diacetyl

Figure 3. Pheromone activates ASK and ADL sensory neurons but inhibits downstream AIA interneurons

(A) Schematic of synaptic connections between ASK, ADL, AWA, AIA.

(B) Top – ADL::*GCaMP6s* (L/R) and Bottom – ASK::*GCaMP6s* (L/R) somatic average traces in response to pheromone delivery in microfluidics device. L4 stage. N=16 animals (ADL) and N=17 animals (ASK). Data represented as mean (thick black line) ± SEM (gray shading).

(C) Dauer formation assays for ADL::*HisCl1* animals grown on plates with and without histamine. N=4-7 population assays. Strain is an extrachromosomal array, only transgenic animals counted. Data represented as mean ± SEM, student's t-test equal variance, **p<0.01.

(D) Dauer formation assays for ASK>*HisCl1* animals grown on plates with and without histamine. N=7-9 population assays. Data represented as mean ± SEM, student's t-test equal variance, ***p<0.001.

(E) AIA::*GCaMP6s* process average trace in response to pheromone delivery in microfluidics device. Only animals with spontaneous activity prior to pheromone delivery shown. L4 stage. N=5 animals. Data represented as mean (thick black line) ± SEM (gray shading).

(F) Dauer formation assays for N2 animals grown in presence of 2 uL ethanol or 2 uL 1:1000 diacetyl diluted in ethanol. N=4 population assays. Data represented as mean ± SEM, student's t-test equal variance, ns=no significance.

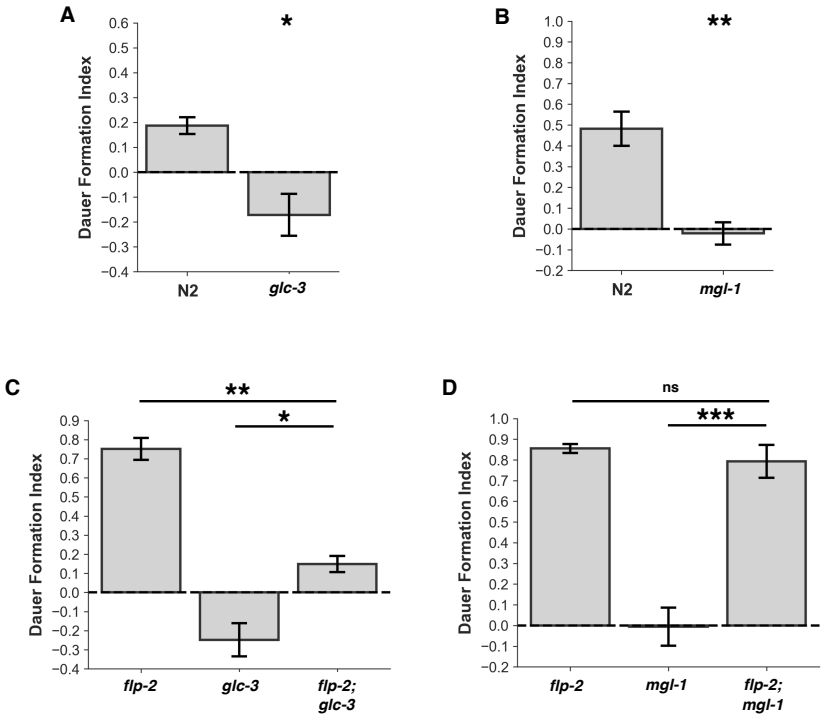

Figure 4. FLP-2 signaling is inhibited by glutamatergic transmission via the metabotropic glutamate receptor MGL-1.

(A) Dauer formation assays for *glc-3* mutants. N=4 population assays. Data represented as mean ± SEM, student's t-test equal variance, *p<0.05.

(B) Dauer formation assays for *mgl-1* mutants. N=5-6 population assays. Data represented as mean ± SEM, student's t-test equal variance, **p<0.01.

(C) Dauer formation assays for *flp-2; glc-3* mutants. N=3-4 population assays. Data represented as mean ± SEM, ANOVA followed by Dunnett's compared to double mutant, *p<0.05, **p<0.01.

(D) Dauer formation assays for *flp-2; mgl-1* mutants. N=3-4 population assays. Data represented as mean ± SEM, ANOVA followed by Dunnett's compared to double mutant, ns=no significance, ***p<0.001.

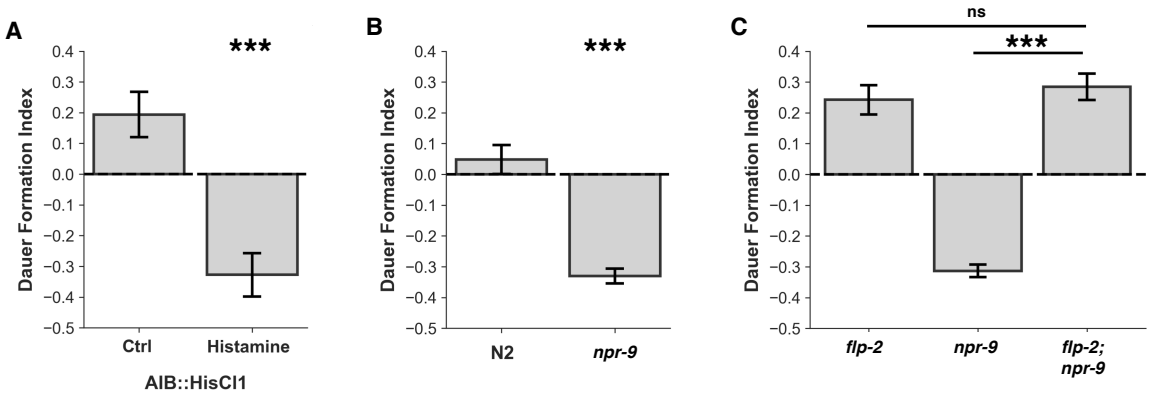

Figure 5. AIB interneurons and their neuropeptide receptor NPR-9 promote diapause entry.

(A) Dauer formation assays for AIB>*HisCl1* animals grown on plates with and without histamine. N=7 population assays. Data represented as mean ± SEM, student's t-test equal variance, ***p<0.001.

(B) Dauer formation assays for *npr-9* mutants. N=4 population assays. Data represented as mean ± SEM, student's t-test equal variance, ***p<0.001.

(C) Dauer formation assays for *flp-2; npr-9* mutants. N=4 population assays. Data represented as mean ± SEM, ANOVA followed by Dunnett's compared to double mutant, **p<0.01.

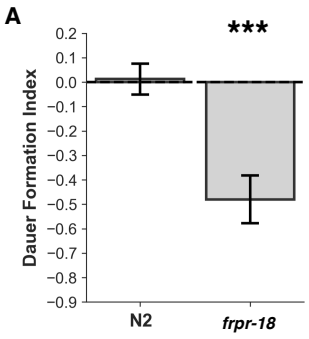
A
***
Dauer Formation Index
N2
frpr-18

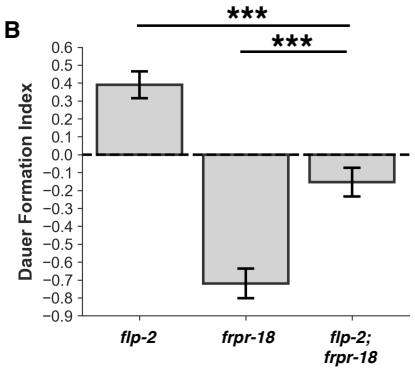
B
***
***
Dauer Formation Index
flp-2
frpr-18
flp-2;
frpr-18

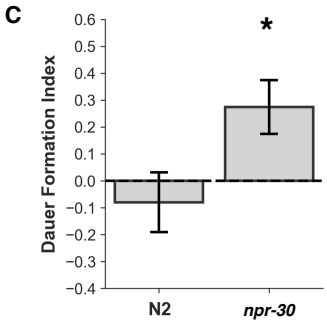
C
*
Dauer Formation Index
N2
npr-30

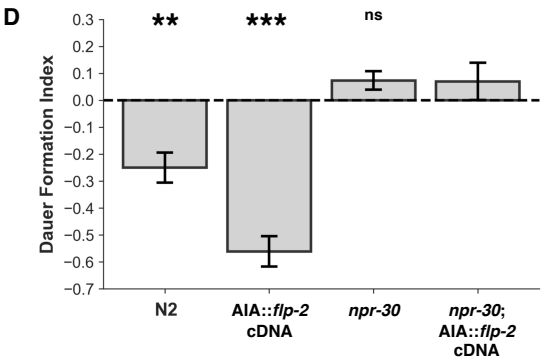
D
**
***
ns
Dauer Formation Index
N2
AIA::flp-2
cDNA
npr-30
npr-30;
AIA::flp-2
cDNA

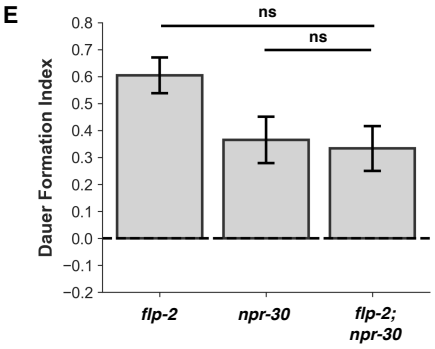
E
ns
ns
Dauer Formation Index
flp-2
npr-30
flp-2;
npr-30

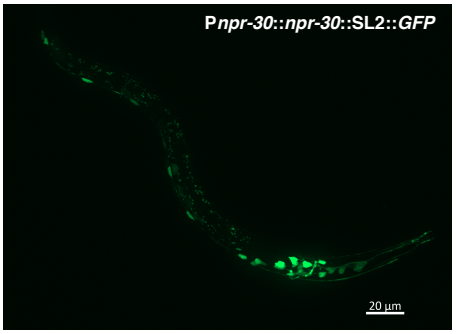
F
Pnpr-30::npr-30::SL2::GFP
20 µm

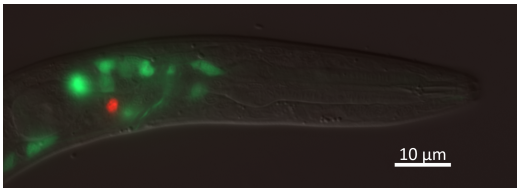
G
10 µm

Figure 6. The broadly-expressed neuropeptide receptor NPR-30 mediates FLP-2 signaling.

(A) Dauer formation assays for *frpr-18* mutants. N=7 population assays. Data represented as mean ± SEM, student's t-test equal variance, ***p<0.001.

(B) Dauer formation assays for *flp-2; frpr-18* mutants. N=7 population assays. Data represented as mean ± SEM, ANOVA followed by Dunnett's compared to double mutant, ***p<0.001.

(C) Dauer formation assays for *npr-30* mutants. N=7-8 population assays. Data represented as mean ± SEM, student's t-test equal variance, *p<0.05.

(D) Dauer formation assays for *npr-30* suppression of AIA::*flp-2* cDNA overexpression. Only transgenic animals counted. N=4-8 population assays. Data represented as mean ± SEM, ANOVA followed by Dunnett's compared to *npr-30*; AIA::*flp-2* cDNA, ns=no significance, **p<0.01, ***p<0.001.

(E) Dauer formation assays for *flp-2; npr-30* mutants. N=3-4 population assays. Data represented as mean ± SEM, ANOVA followed by Dunnett's compared to double mutant, ns=no significance.

(F) Image of *npr-30* translational GFP reporter expression in an L1 stage larva. Mosaic animal with GFP in neurons only.

(G) Merged channels image of AIA::*mCherry-H2B* and *npr-30* translational GFP reporter in an L1 stage larva.

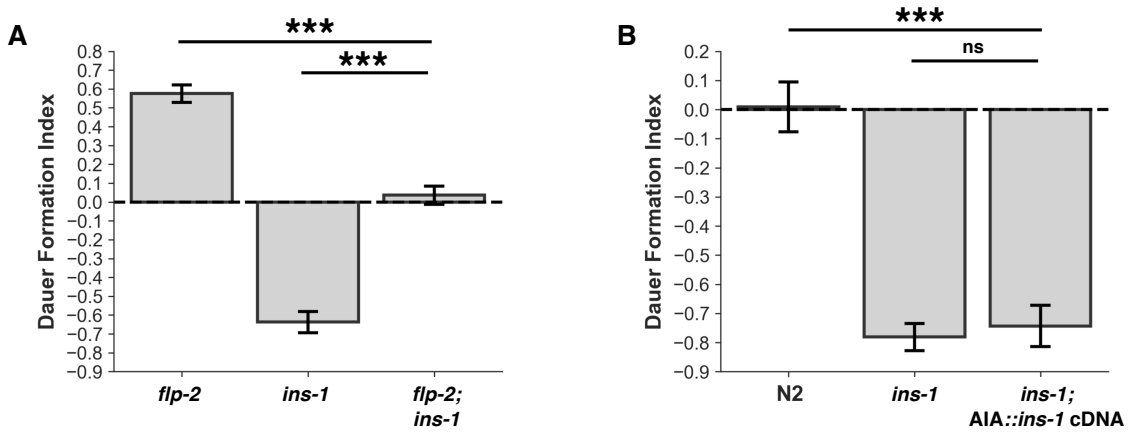

Figure 7. INS-1 and FLP-2 have antagonistic roles in developmental decision-making.

(A) Dauer formation assays for *flp-2; ins-1* mutants. N=3-4 population assays. Data represented as mean ± SEM, ANOVA followed by Dunnett's compared to double mutant, ***p<0.001.

(B) Dauer formation assays for AIA-specific *ins-1* cDNA expression in *ins-1* mutants. N=4 population assays. Data represented as mean ± SEM, ANOVA followed by Dunnett's compared to N2, ***p<0.001.

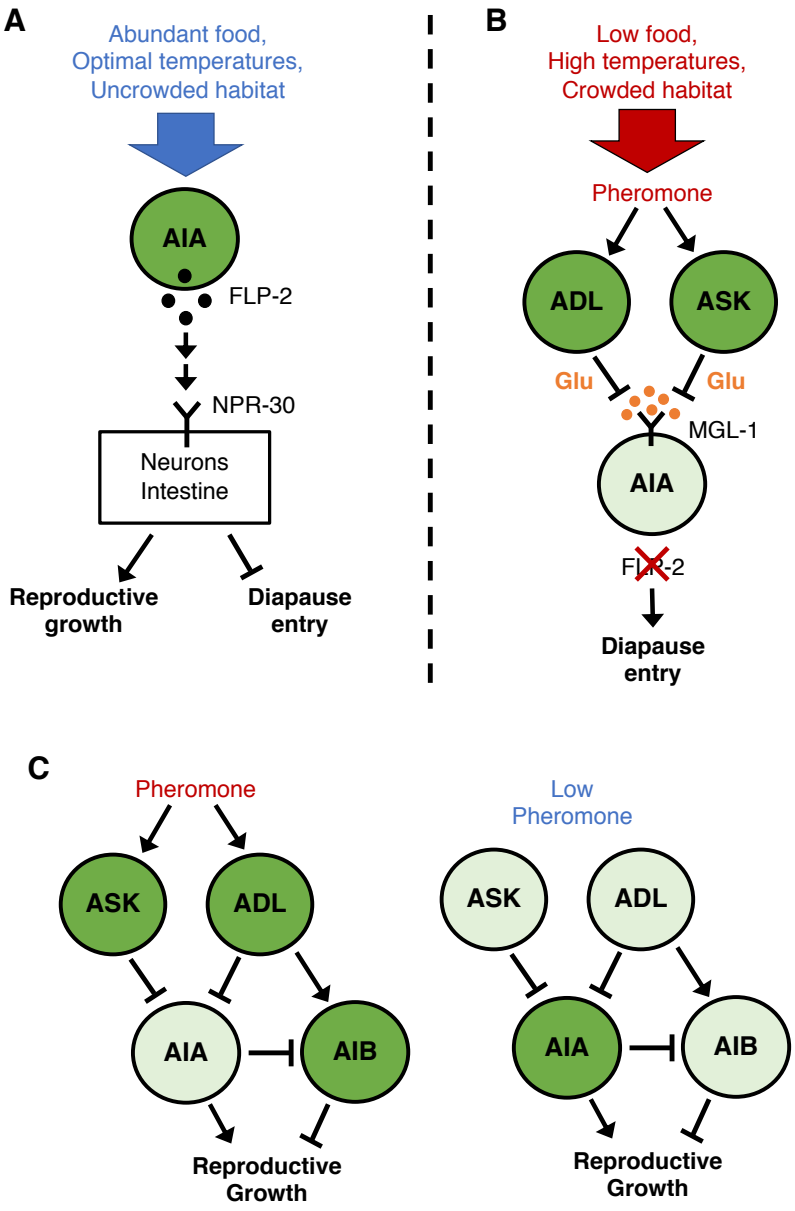

Figure 8: AIA controls a neuropeptide switch between different larval developmental trajectories.

(A and B) Schematic model of AIA-derived FLP-2 signaling pathways under different environmental conditions: (A) Reproductive growth conditions and (B) Dauer-inducing conditions.

(C) Schematic model of neural circuit mediating the diapause entry decision including pheromone-sensing neurons and interneurons identified in this study.

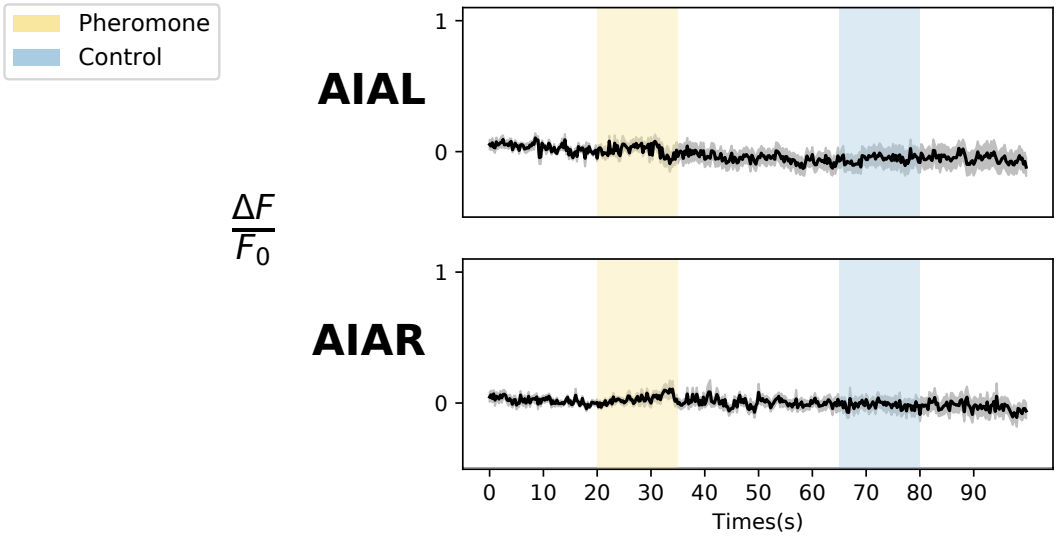

Supplementary Figure 1. AIA soma GCaMP response to pheromone delivery.

AIA::*GCaMP6s* (L/R) somatic average traces in response to pheromone delivery in microfluidics device. L4 stage. N=14 animals. Data represented as mean (thick black line) ± SEM (gray shading).

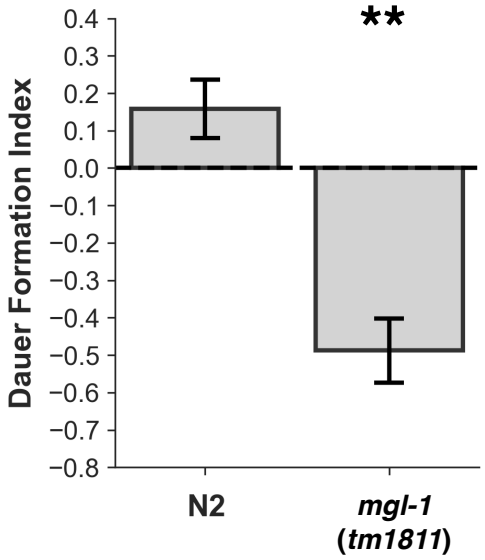

Supplementary Figure 2. *mgl-1*(*tm1811*) deletion allele has a decreased dauer formation phenotype.

Dauer formation assays for *mgl-1*(*tm1811*) mutants. N=4 population assays. Data represented as mean ± SEM, student's t-test equal variance, **p<0.01.

2.6 Materials and Methods

Animal maintenance and strains

Animals were cultivated at 21°C on standard nematode growth media (NGM) plates seeded with *Escherichia coli* OP50 cultured in Luria-Bertani(LB) broth. The following strains were used in this study:

N2 (Bristol)

PS9101: *syIs759*[P*gcy-28*.d::*HisCl1*::SL2::*GFP*, P*flp-2*::*flp-2* cDNA::*mCherry*, P*ofm-1*::*GFP*]

PS7370: *flp-2*(*ok3351*)

PS8968: *flp-2*(*ok3351*); *syEx1755*[P*flp-2*::*flp-2* cDNA::SL2::*GFP*, P*ofm-1*::*RFP*]

PS9150: *flp-2*(*ok3351*); *syEx1866*[P*ges-1*::*flp-2* cDNA::SL2::*GFP*, P*ofm-1*::*RFP*]

PS8735: *syEx1755*[P*flp-2*::*flp-2* cDNA::SL2::*GFP*, P*ofm-1*::*RFP*]

PS7866: *syIs493*[P*sra-9*::*cGAL*, P*ofm-1*::*RFP*]; *syIs371*[*UAS*::*HisCl1*::SL2::*GFP*, P*ofm-1*::*GFP*]

PS9006: *syEx1811*[P*sre-1*::*HisCl1*::SL2::*GFP*, P*ofm-1*::*RFP*]

PS8955: *syEx1793*[P*sra-9*::*GCaMP6s*, P*sre-1*::*GCaMP6s*, P*gcy-28*.d::*GCaMP6s*]

PS9111: *syIs761*[P*gcy-28*.d::*GCaMP6s*, P*myo-2*::*mCherry*]

RB594: *glc-3*(*ok321*)

PS9220: *flp-2*(*ok3351*); *glc-3*(*ok321*)

PS8586: *npr-9*(*sy1417*)

PS8628: *flp-2*(*ok3351*); *npr-9*(*sy1429*)

PS8159: *syIs540*[P*npr-9*::*cGAL*, P*ofm-1*::*RFP*]; *syIs371*[*UAS*::*HisCl1*::SL2::*GFP*, P*ofm-1*::*GFP*]

PS9192: *mgl-1*(*sy1623*)

PS9193: *flp-2*(*ok3351*); *mgl-1*(*sy1624*)

PS7624: *frpr-18*(*ok2698*)

PS7831: *flp-2*(*ok3351*); *frpr-18*(*ok2698*)

FX06617: *npr-30*(*tm6617*)

PS8608: *flp-2*(*ok3351*); *npr-30*(*tm6617*)

PS8931: *npr-30*(*tm6617*); *syEx1755*[P*flp-2*::*flp-2* cDNA::SL2::*GFP*, P*ofm-1*::*RFP*]

FX01888: *ins-1*(*tm1888*)

PS9137: *flp-2*(*ok3351*); *ins-1*(*tm1888*)

PS9147: *ins-1*(*tm1888*); *syEx1863*[P*gcy-28*.d::*ins-1* cDNA::SL2::*mCherry-H2B*, P*ofm-1*::*RFP*]

PS9152: *npr-30*(*tm6617*); *syEx1868*[P*npr-30*::*npr-30* genomic DNA::SL2::*GFP*, P*gcy-28*.d::*mCherry-H2B*, P*ofm-1*::*RFP*]

PS8919: *syEx1777*[P*flp-2*::*GFP*, P*gcy-28*.d::*mCherry-H2B*, P*ofm-1*::*RFP*]

Molecular biology and transgenesis

flp-2 and ins-1 cDNA was PCR amplified from N2 cDNA library. Promoters and *npr-30* genomic DNA were PCR amplified from N2 genomic DNA library. *Drosophila HisCl1* was PCR amplified from pJL046. Constructs were inserted into pSM *GFP*, pSM *mCherry-H2B* or pSM *GCaMP6s* vector backbone using HiFi Assembly or restriction cloning.

Transgenic strains were generated by microinjection of plasmids with co-injection markers into adult worms. Plasmids were injected at 10-50 ng/uL. Co-injection markers were injected at: P*myo-2*::*mCherry* (0.5 ng/uL), P*ofm-1*::*RFP* (40 ng/uL), P*ofm-1*::*GFP* (30-40 ng/uL). 1 kb DNA ladder was used as a filler to bring final DNA concentration to 200 ng/uL.

CRISPR mutagenesis

CRISPR mutagenesis was performed as described in Wang *et al.* 2018[57]. Briefly, a 43-base-pair universal STOP-IN cassette was inserted near the 5' end of the target gene to disrupt translation. Independent F1 homozygous animals were isolated using PCR detection and confirmed with sequencing.

Pheromone-induced dauer formation assays

Crude dauer pheromone extract was obtained as described in Schroeder and Flatt 2014[58]. Dauer formation assay protocol was performed as described in Lee *et al*. 2017[12]. Heat-killed OP50 was made by washing bacteria from an overnight culture with virgin S-basal, resuspending with virgin S-basal, and killing at 95-100°C. The afternoon before

experiments, L4 worms were picked from well-fed stock plates onto seeded plates and grown overnight at 21°C. Pheromone of desired volume was placed at the center of 35 mm Petri dishes and 2 mL of NGM agar without peptone was poured into each plate. Plates were dried overnight on benchtop at 21°C. On the day of experiments, pheromone plates were seeded with 2 uL heat-killed OP50 and adults animals were allowed to lay 60-70 eggs per plate. Adults were then picked off and 18 uL of heat-killed OP50 added to the plates. Once the food patch had completely dried, plates were parafilmed and placed in a 25.5°C incubator for 72 hours. The number of dauers and non-dauers per plate were counted and the Dauer Formation Index (DFI) per plate calculated using the following formula:

$$\text{DFI} = \frac{\text{No. of Dauers} - \text{No. of Non-dauers}}{\text{No. of Dauers} + \text{No. of Non-dauers}}$$

To make histamine plates, histamine dihydrochloride powder was mixed into NGM agar at ~50°C to a final concentration of 10 mM and poured into plates.

For dauer formation assays with diacetyl, assays were set up as described above. Before parafilming, 2 uL of 200 proof ethanol or 2 uL or 1:1000 diacetyl diluted in ethanol was added to the side of the food patch.

For experiments that used extrachromosomal array lines, lines that had 70-80% array transmission rates were selected for population assays. All animals on each plate were counted unless noted otherwise. At least 3 population assays were completed for each control and genotype/treatment, with each assay containing 60-70 worms. Control and genotype/treatment plates were always assayed simultaneously under the same conditions for comparisons. All statistical analyses were performed in R Studio.

Microscopy

Animals were immobilized with 10 mM sodium azide on 2% agarose pads. Slides were imaged under a ZEISS Imager.Z2 microscope attached to a Axiocam 506 mono camera capture source. Images were processed using ZenPro software.

Pheromone delivery in microfluidics device

Microfluidic device fabrication

We designed a 2-layer microfluidic chip capable of delivering sequences of stimuli with a worm trap suitable for housing worms at L4 larval stage. The chip was designed in AutoCAD software, and sent to CAD/Art Services, Inc to print the photomask. Photolithography in a clean room was performed on a silicon wafer to make the 2-layer mold from the photomask. For the first layer, which included the worm trap, SU-8 2025 was spin coated on the silicon wafer at 4000 *rpm* to achieve 25 μm thickness. For the second layer, the same photoresist was spin coated at 1250 *rpm* for a thickness of 70 μm. Polydimethylsiloxane (PDMS) was poured over the mold and cured on a 90$^{\circ}C$ hotplate to solidify. Each PDMS chip was then punched with a 1 *mm* biopsy punch and was bonded to a cover slip using a handheld corona treater.

Microfluidic experiment design

Our chip design was a modified version of the microfluidic chip used in Chronis *et al.* 2007[59]. It has 13 channels for different odorants and soluble chemicals, one channel for buffer and two channels to control the direction of the flow. At every moment, one of the stimuli channels and one of the control channels are on, and the buffer channel is always on. If control-1 is on and control-2 is off then buffer is delivered to the worm and if the control channels are switched, stimulus will be delivered to the worm. Since controls will never touch the worm, choice of controls is not crucial, here water was used. To deliver the stimuli and control the timing of each delivery, microfluidic chip was connected to a set of syringes filled with odors and buffers by thin tubing. All syringes were connected to a pressure control system that regulated the laboratory's air pressure.The system provided enough pressure for the liquid to flow inside the tubing. Tubing that came out of each syringe went through a pinch valve, which then was connected to a controller used to turn valves on and off. Custom software written in Python sent signals to the controller via a DAQ device to switch each valve. This ensured precise timing of odor and buffer delivery, and was synchronized with the imaging system. Every time a valve switched, it was logged and later used in data analysis. We chose 3 stimuli for the experiment. 12% (v/v) diluted crude pheromone extract in CTX buffer (5

mL 1M KPO4, 1 mL 1M MgSO4, 1 mL 1M CaCl2, 2.922 gNaCl, 993 mL mili-Q water) as the main stimulus, 0.01 mM Fluorescein to confirm chemical delivery, and CTX buffer as a control buffer. Each stimulus interval was 15 seconds, enough time to capture the rise and fall of calcium transients. Stimulus interval was then followed by a 30-second buffer interval to give neurons enough time to return to baseline and be ready for the next stimulus. L4 stage animals were used in all assays. For Figure 3B and Figure S1, the average response during the 5 seconds before pheromone delivery was used as a baseline to plot delta(F)/F0. For Figure 3E, the average of the first 5 seconds of each trace was used as a baseline to plot delta(F)/F0.

2.7 References

1. Kelly, S. A., Panhuis, T. M. & Stoehr, A. M. Phenotypic plasticity: Molecular mechanisms and adaptive significance. *Compr. Physiol.* (2012). doi:10.1002/cphy.c110008
2. Beldade, P., Mateus, A. R. A. & Keller, R. A. Evolution and molecular mechanisms of adaptive developmental plasticity. *Molecular Ecology* (2011). doi:10.1111/j.1365-294X.2011.05016.x
3. Ghosh, S. M., Testa, N. D. & Shingleton, A. W. Temperature-size rule is mediated by thermal plasticity of critical size in Drosophila melanogaster. *Proceedings of the Royal Society B: Biological Sciences* (2013). doi:10.1098/rspb.2013.0174
4. Lafuente, E., Duneau, D. & Beldade, P. Genetic basis of thermal plasticity variation in Drosophila melanogaster body size. *PLoS Genet.* (2018). doi:10.1371/journal.pgen.1007686
5. Trotta, V. *et al.* Thermal plasticity in Drosophila melanogaster: A comparison of geographic populations. *BMC Evol. Biol.* (2006). doi:10.1186/1471-2148-6-67
6. Nussey, D. H., Kruuk, L. E. B., Morris, A. & Clutton-Brock, T. H. Environmental conditions in early life influence ageing rates in a wild population of red deer. *Current Biology* (2007). doi:10.1016/j.cub.2007.10.005
7. Albon, S. D., Clutton-Brock, T. H. & Guinness, F. E. Early Development and Population Dynamics in Red Deer. II. Density-Independent Effects and Cohort Variation. *J. Anim. Ecol.* (1987). doi:10.2307/4800
8. Laforsch, C. & Tollrian, R. Inducible defenses in multipredator environments: Cyclomorphosis in Daphnia cucullata. *Ecology* (2004). doi:10.1890/03-0286
9. Pijanowska, J. Anti-predator Defence in Three Daphnia Species. *Int. Rev. der gesamten Hydrobiol. und Hydrogr.* (1992). doi:10.1002/iroh.19920770111
10. Golden, J. W. & Riddle, D. L. The Caenorhabditis elegans dauer larva: Developmental effects of pheromone, food, and temperature. *Dev. Biol.* (1984). doi:10.1016/0012-1606(84)90201-X
11. Cassada, R. C. & Russell, R. L. The dauerlarva, a post-embryonic developmental variant of the nematode Caenorhabditis elegans. *Dev. Biol.* **46**, 326–342 (1975).
12. Lee, J. S. *et al.* FMRFamide-like peptides expand the behavioral repertoire of a densely connected nervous system. *Proc. Natl. Acad. Sci. U. S. A.* (2017). doi:10.1073/pnas.1710374114
13. Lee, H. *et al.* Nictation, a dispersal behavior of the nematode Caenorhabditis elegans, is regulated by IL2 neurons. *Nat. Neurosci.* (2012). doi:10.1038/nn.2975
14. Hallem, E. A. *et al.* A sensory code for host seeking in parasitic nematodes. *Curr. Biol.* (2011). doi:10.1016/j.cub.2011.01.048
15. Bhattacharya, A., Aghayeva, U., Berghoff, E. G. & Hobert, O. Plasticity of the Electrical Connectome of C. elegans. *Cell* (2019). doi:10.1016/j.cell.2018.12.024
16. Klass, M. & Hirsh, D. Non-ageing developmental variant of Caenorhabditis elegans. *Nature* (1976). doi:10.1038/260523a0
17. Golden, J. W. & Riddle, D. L. A pheromone influences larval development in the nematode Caenorhabditis elegans. *Science (80-.).* (1982).

doi:10.1126/science.6896933

18. Butcher, R. A., Ragains, J. R., Kim, E. & Clardy, J. A potent dauer pheromone component in Caenorhabditis elegans that acts synergistically with other components. *Proc. Natl. Acad. Sci. USA* **105**, 14288–14292 (2008).
19. Jeong, P. *et al.* Chemical structure and biological activity of the Caenorhabditis elegans dauer-inducing pheromone. *Nature* **433**, 541–545 (2005).
20. Pungaliya, C. *et al.* A shortcut to identifying small molecule signals that regulate behavior and development in Caenorhabditis elegans. *Proc. Natl. Acad. Sci. U. S. A.* (2009). doi:10.1073/pnas.0811918106
21. McGrath, P. T. *et al.* Parallel evolution of domesticated Caenorhabditis species targets pheromone receptor genes. *Nature* **477**, 321–325 (2011).
22. Kim, K. *et al.* Two Chemoreceptors Mediate Developmental Effects of Dauer Pheromone in C. elegans. *Science (80-.).* **326**, 994–998 (2009).
23. Schackwitz, W. S., Inoue, T. & Thomas, J. H. Chemosensory neurons function in parallel to mediate a pheromone response in C. elegans. *Neuron* **17**, 719–728 (1996).
24. Bargmann, C. I. & Horvitz, H. R. Control of larval development by chemosensory neurons in Caenorhabditis elegans. *Science* **251**, 1243–6 (1991).
25. Szø, J. Y., Victor, M., Loer, C., Shi, Y. & Ruvkun, G. Food and metabolic signalling defects in a Caenorhabditis elegans serotonin-synthesis mutant. *Nature* (2000). doi:10.1038/35000609
26. Faumont, S., Lindsay, T. H. & Lockery, S. R. Neuronal microcircuits for decision making in C. elegans. *Current Opinion in Neurobiology* **22**, 580–591 (2012).
27. White, J. G., Southgate, E., Thomson, J. N. & Brenner, S. The structure of the nervous system of the nematode Caenorhabditis elegans. *Philos. Trans. R. Soc. Lond. B. Biol. Sci.* **314**, 1–340 (1986).
28. Pokala, N., Liu, Q., Gordus, A. & Bargmann, C. I. Inducible and titratable silencing of Caenorhabditis elegans neurons in vivo with histamine-gated chloride channels. *Proc. Natl. Acad. Sci. U. S. A.* (2014). doi:10.1073/pnas.1400615111
29. Chase, D. L. & Koelle, M. R. Biogenic amine neurotransmitters in C. elegans. *WormBook : the online review of C. elegans biology* (2007). doi:10.1895/wormbook.1.132.1
30. Kim, K. & Li, C. Expression and regulation of an FMRFamide-related neuropeptide gene family in Caenorhabditis elegans. *J. Comp. Neurol.* (2004). doi:10.1002/cne.20189
31. Shinkai, Y. *et al.* Behavioral choice between conflicting alternatives is regulated by a receptor guanylyl cyclase, GCY-28, and a receptor tyrosine kinase, SCD-2, in AIA interneurons of Caenorhabditis elegans. *J. Neurosci.* **31**, 3007–3015 (2011).
32. Fares, H. & Greenwald, I. Genetic analysis of endocytosis in caenorhabditis elegans: Coelomocyte uptake defective mutants. *Genetics* (2001). doi:10.1093/genetics/159.1.133
33. Macosko, E. Z. *et al.* A hub-and-spoke circuit drives pheromone attraction and social behaviour in C. elegans. *Nature* **458**, 1171–1175 (2009).
34. Chen, T. W. *et al.* Ultrasensitive fluorescent proteins for imaging neuronal activity. *Nature* (2013). doi:10.1038/nature12354
35. Hendricks, M. Compartmentalized calcium dynamics in a C. elegans interneuron

encode head movement. *Nature* (2012). doi:10.1038/nature11081

36. Bargmann, C. I., Hartwieg, E. & Horvitz, H. R. Odorant-selective genes and neurons mediate olfaction in C. elegans. *Cell* **74**, 515–527 (1993).
37. Dobosiewicz, M., Liu, Q. & Bargmann, C. I. Reliability of an interneuron response depends on an integrated sensory state. *Elife* (2019). doi:10.7554/eLife.50566
38. Serrano-Saiz, E. *et al.* XModular control of glutamatergic neuronal identity in C. elegans by distinct homeodomain proteins. *Cell* **155**, 659 (2013).
39. Horoszok, L., Raymond, V., Sattelle, D. B. & Wolstenholme, A. J. GLC-3: A novel fipronil and BIDN-sensitive, but picrotoxinin-insensitive, L-glutamate-gated chloride channel subunit from Caenorhabditis elegans. *Br. J. Pharmacol.* (2001). doi:10.1038/sj.bjp.0703937
40. Dillon, J., Hopper, N. A., Holden-Dye, L. & O'Connor, V. Molecular characterization of the metabotropic glutamate receptor family in Caenorhabditis elegans. *Biochem. Soc. Trans.* (2006). doi:10.1042/BST0340942
41. Chen, D., Taylor, K. P., Hall, Q. & Kaplan, J. M. The neuropeptides FLP-2 and PDF-1 act in concert to arouse Caenorhabditis elegans locomotion. *Genetics* **204**, 1151–1159 (2016).
42. Wenick, A. S. & Hobert, O. Genomic cis-regulatory architecture and trans-acting regulators of a single interneuron-specific gene battery in C. elegans. *Dev. Cell* (2004). doi:10.1016/j.devcel.2004.05.004
43. Jeong, H. & Paik, Y. K. MGL-1 on AIY neurons translates starvation to reproductive plasticity via neuropeptide signaling in Caenorhabditis elegans. *Dev. Biol.* (2017). doi:10.1016/j.ydbio.2017.08.014
44. Bendena, W. G. *et al.* A Caenorhabditis elegans allatostatin/galanin-like receptor NPR-9 inhibits local search behavior in response to feeding cues. *Proc. Natl. Acad. Sci. U. S. A.* **105**, 1339–1342 (2008).
45. Larsen, M. J. *et al.* Functional expression and characterization of the C. elegans G-protein-coupled FLP-2 Receptor (T19F4.1) in mammalian cells and yeast. *Int. J. Parasitol. Drugs Drug Resist.* **3**, 1–7 (2013).
46. Taylor, S. R. *et al.* Molecular topography of an entire nervous system. *bioRxiv* (2020). doi:10.1101/2020.12.15.422897
47. Kodama, E. *et al.* Insulin-like signaling and the neural circuit for integrative behavior in C. elegans. *Genes Dev.* (2006). doi:10.1101/gad.1479906
48. Chalasani, S. H. *et al.* Neuropeptide feedback modifies odor-evoked dynamics in Caenorhabditis elegans olfactory neurons. *Nat. Neurosci.* **13**, 615–621 (2010).
49. Pierce, S. B. *et al.* Regulation of DAF-2 receptor signaling by human insulin and ins-1, a member of the unusually large and diverse C. elegans insulin gene family. *Genes Dev.* (2001). doi:10.1101/gad.867301
50. Turek, M., Besseling, J. & Bringmann, H. Agarose Microchambers for Long-term Calcium Imaging of Caenorhabditis elegans *J. Vis. Exp.* (2015). doi:10.3791/52742
51. Bringmann, H. Agarose hydrogel microcompartments for imaging sleep- and wake-like behavior and nervous system development in Caenorhabditis elegans larvae. *J. Neurosci. Methods* (2011). doi:10.1016/j.jneumeth.2011.07.013
52. López-Cruz, A. *et al.* Parallel Multimodal Circuits Control an Innate Foraging

Behavior. *Neuron* (2019). doi:10.1016/j.neuron.2019.01.053

53. Durand, D., Pampillo, M., Caruso, C. & Lasaga, M. Role of metabotropic glutamate receptors in the control of neuroendocrine function. *Neuropharmacology* (2008). doi:10.1016/j.neuropharm.2008.06.022
54. Cartmell, J. & Schoepp, D. D. Regulation of neurotransmitter release by metabotropic glutamate receptors. *Journal of Neurochemistry* (2000). doi:10.1046/j.1471-4159.2000.0750889.x
55. Saper, C. B. & Lowell, B. B. The hypothalamus. *Current Biology* (2014). doi:10.1016/j.cub.2014.10.023
56. Scaccianoce, S. *et al.* Endogenous activation of group-II metabotropic glutamate receptors inhibits the hypothalamic-pituitary-adrenocortical axis. *Neuropharmacology* (2003). doi:10.1016/S0028-3908(03)00027-3
57. Wang, H., Park, H., Liu, J. & Sternberg, P. W. An efficient genome editing strategy to generate putative null mutants in Caenorhabditis elegans using CRISPR/Cas9. *G3 Genes, Genomes, Genet.* (2018). doi:10.1534/g3.118.200662
58. Schroeder, N. E. & Flatt, K. M. In vivo imaging of Dauer-specific neuronal remodeling in C. elegans. *J. Vis. Exp.* e51834 (2014). doi:10.3791/51834
59. Chronis, N., Zimmer, M. & Bargmann, C. I. Microfluidics for in vivo imaging of neuronal and behavioral activity in Caenorhabditis elegans. *Nat. Methods* (2007). doi:10.1038/nmeth1075

CHAPTER 3: FKH-7/FOXP regulates sensory neuron function during developmental decision-making

3.1 Abstract

The FoxP subfamily of transcription factors are critical regulators of development in many vital tissues including the nervous system, heart, and lungs. In mouse and fly models, consequences of FoxP activity loss in the brain include altered neuron morphology and excitability resulting in behavioral deficits. Despite *C. elegans*' tractability for molecular and cellular investigations, the function of the sole *C. elegans* ortholog of FoxP, FKH-7, has never been studied. Here, we discover and characterize a role for FKH-7 in regulating sensory neuron function during developmental decision-making. We show that FKH-7 is required in both the ADL and ADF sensory neurons to promote diapause entry under pheromone dauer-inducing conditions and that human FOXP1 can functionally substitute for FKH-7 in this developmental context. We also show that loss of FKH-7 activity does not disrupt sensory neuron morphology and spatial localization within the nerve ganglia. Finally, we find that the autism spectrum disorder-associated *fkh-7*(R612C) and *fkh-7*(R563G) missense variants also have a reduction in dauer formation phenotype. Our results reveal a novel function for the conserved transcription factor FKH-7/FOXP in regulating sensory control of developmental plasticity when challenged with stressful stimuli.

3.2 Introduction

The evolutionarily-conserved forkhead box (Fox) family of transcription factors are characterized by a winged-helix DNA-binding domain (DBD) and can be found in organisms as diverse as animals, fungi, and related protists[1]. In animals, many of them have important biological functions in development as well as during adulthood. The dysfunction of many Fox members has been implicated in a variety of human diseases and disorders such as cancer, autism spectrum disorder, speech language defects, congenital heart disease, and immune regulation deficiencies[2–7]. Despite the clinical-relevance of mouse models, complete loss of critical Fox developmental regulators often leads to embryonic lethality[8–12]. In addition, their relatively long life cycles and physiological complexity usually precludes systematic *in vivo* dissections of Fox-mediated gene regulatory networks. Although *C. elegans* has only 15 Fox genes compared to 44 in humans, studies in the roundworm have played a pivotal role in identifying conserved Fox targets, elucidating the mechanism of their molecular interactions, and characterizing the signaling pathways they regulate[13–16]. One notable example is lifespan extension by the well-studied *C. elegans* DAF-16/FOXO transcription factor which primarily acts in the intestine to regulate metabolic processes[17–20]. In response to stressful environmental conditions, decreased expression of the insulin receptor-like DAF-2 results in translocation of unphosphorylated DAF-16 into the nucleus where it regulates the expression of downstream targets that promote development into the protective, long-lived dauer stage[21,22].

The FoxP subfamily of transcription factors has four paralogs in mammals – *FoxP1*, *FoxP2*, *FoxP3*, and *FoxP4*. While all four have reported roles in human disease, only *FOXP1* and *FOXP2* have been implicated in cognitive developmental disorders. In particular, mutations in *FOXP1* and *FOXP2* are associated with speech and language acquisition deficits, intellectual disability, and autism spectrum disorder[23–26]. Although the molecular consequences of these mutations and how they subsequently lead to neural dysfunction remains poorly understood, their phenotypic consequences are being increasingly documented in model organisms. In zebra finches, knockdown of *Foxp2* expression during adolescence decreased song-learning precision[27]. Brain-specific *Foxp1* knockout in mice resulted in abnormal morphogenesis and reduced excitability of hippocampal CA1 region cells as well as increased striatal dendritic branching *in vitro*[28]. Furthermore, the orthologous *FoxP* in flies mediates the accuracy of perceptual decision-making by downregulating the voltage-gated potassium channel Shal in mushroom body Kenyon cells[29,30]. Despite the array of cognitive and behavioral functions regulated by the FoxPs in disparate organisms, the function of their sole worm ortholog

FKH-7 has never been studied. Here, we discover and characterize a role for this evolutionarily-conserved transcription factor in regulating *C. elegans* sensory neuron function in the context of a developmental decision-making paradigm.

3.3 Results

FKH-7 is required for pheromone-induced diapause entry

There are fourteen predicted *fkh-7* protein-coding transcripts but no pre-existing mutant reagents that disrupt all of them. To obtain such a mutation, we used a CRISPR-based strategy to delete genomic regions that encode the conserved transcription factor DNA-binding domain. We generated two new *fkh-7* alleles – the *sy1575* allele harbors a 1.26 kb in-frame deletion nested within the forkhead domain-encoding region while the *sy1576* allele harbors a 1.5 kb in-frame deletion that removes the first half of the forkhead domain-encoding region together with most of the preceding exon. Both *fkh-7* deletion alleles exhibited a significant reduction in dauer formation under pheromone dauer-inducing conditions with the larger *sy1576* deletion resulting in a more severe phenotype (Figure 1A). We also assayed the *fkh-7*(*tm6093*) mutant which has a premature stop codon in the region encoding the coiled-coil domain that truncates eight of the longest predicted *fkh-7* transcripts. This particular mutant had a decreased dauer formation phenotype that was similar in magnitude to the *sy1576* deletion suggesting that loss of the longer *fkh-7* transcripts might account for the *fkh-7*(*sy1576*) phenotype (Figure 1B).

To determine the spatiotemporal expression pattern of *fkh-7*, we fused 4 kb of upstream regulatory sequence 5' to the *fkh-7*.a transcript start codon to GFP and imaged transgenic larvae at different life stages along the reproductive and dauer developmental trajectories. During the L1 stage, *fkh-7*.a expression is localized to a few neurons in the head and tail as well as in the intestine (Figure 2A). After the L1 stage, *fkh-7*.a expression patterns diverge as larvae develop under different growth conditions. Under reproductive growth conditions, GFP expression in L2 and L3 larvae resembles the L1 stage except with dimmer intestine expression (Figure 2B,C). GFP intensity in neurons and the intestine increases during the pre-dauer L2d stage before becoming widespread in several tissues in dauers (Figure 2D,E). The brighter and more widespread GFP expression during the dauer stages

compared to reproductive development is consistent with *fkh-7* stage-specific whole animal RNA-seq data[31].

FKH-7.a acts in a subset of sensory neurons and the intestine to promote diapause entry

To identify *fkh-7*'s site of action, we used tissue-specific promoters to selectively express *fkh-7*.a cDNA in the *fkh-7*(*sy1576*) mutant. *fkh-7*.a cDNA expression in the intestine and nervous system rescued the *fkh-7* mutant phenotype, but not expression in the body wall muscle, pharyngeal muscle or hypodermis (Figure 3A). We observed that GFP-labelled neurons in our transcriptional reporter had processes that extended to the tip of the animal's nose indicating that these are likely to be amphid sensory neurons. *tax-4* encodes a subunit of the cyclic nucleotide-gated channel TAX-4/TAX-2 while *ocr-2* encodes a subunit of the transient receptor potential channel TRPV[32,33]. We leveraged the fact that their promoters drive expression in complementary subsets of the amphid sensory neurons to narrow down *fkh-7* site of action in the nervous system[32,33]. Expression of *fkh-7*.a cDNA driven by the *ocr-2* promoter rescued the *fkh-7* mutant phenotype while expression in *tax-4* promoter subset did not (Figure 3B). Although an *ocr-2* translational reporter expresses GFP in six neuron classes (ADL, ADF, AWA, ASH, PHA, and PHB)[33], an *ocr-2* transcriptional GFP reporter is only detected in five neuron classes (ADL, ADF, ASH, PHA, and PHB) (Figure 3C).

During the L1 stage, P*fkh-7*.a::GFP and P*ocr-2*::*mCherry-H2B* expression colocalized in the ADL, ADF, and PHB neuron classes (Figure 4A). We first attempted to rescue the fkh-7 mutant phenotype by selectively expressing *fkh-7*.a cDNA using individual neuron class-specific promoters. Neither ADL-specific, ADF-specific, nor ASH+PHA+PHB-specific expression affected the *fkh-7* mutant phenotype (Figure 4B,C,D). However, we found that co-expression of *fkh-7*.a cDNA in both ADL and ADF was sufficient to rescue the *fkh-7* mutant phenotype (Figure 4E). Interestingly, the chemosensory ADL and ADF neurons have antagonistic roles in dauer formation – ADL promotes diapause entry while ADF inhibits it[34,35].

Loss of FKH-7 activity does not disrupt sensory neuron morphology or spatial localization

We next sought to determine how loss of FKH-7 transcription factor activity leads to altered sensory neuron function. One plausible mechanism is that loss of FKH-7 activity affects cell body spatial positioning and/or dendrite outgrowth during embryonic development. To probe this possibility, we first examined P*ocr-2*::*GFP* expression in *fkh-7* mutants during the L1 stage. The positions of all five neuron classes labelled by this construct are unperturbed in the mutant indicating that aberrant anatomical localization does not account for defective neuron function (Figure 5A). In *C. elegans*, the amphid chemosensory neurons extend their dendrites to the animal's nose tip where their dendritic endings terminate in ciliated structures that interface with the external environment. The ciliated endings of some chemosensory neuron class including ADF and ADL possess unique structures that enable identification by visual inspection[36]. Visualization of ADL dendritic projections and ciliated endings using a neuron class-specific GFP reporter show that this aspect of ADL neuron class identity is preserved in *fkh-7* mutants (Figure 5B). ADF dendritic projection pattern and ciliated ending morphology is also preserved in *fkh-7* mutants (Figure 5C).

ASD-associated *fkh-7* missense variants have a decreased dauer formation phenotype

Large-scale comparative analysis of transcription factor regulatory networks indicate that *in vivo* binding sequence preferences of orthologous transcription factor families are largely conserved[37]. We wondered if this generalized principle also holds true for FKH-7/FOXP. We found that human *FOXP1* cDNA expression in the *ocr-2* promoter subset of sensory neurons can functionally substitute for defective FKH-7 and rescued the mutant's dauer formation phenotype (Figure 6A). As a control, we also expressed deficient *FOXP1*(R514C) cDNA that has an altered conserved binding residue in the forkhead domain which did not rescue the *fkh-7* mutant phenotype (Figure 6A)[38].

Advances in patient whole exome sequencing has uncovered many ASD-associated missense variants. A current biomedical challenge is uncovering precisely how these mutations affect gene product function and subsequently disrupt signaling pathways *in vivo*.

Many *FOXP1* ASD-related missense mutations are clustered in genomic regions that encode the functionally-significant, conserved DNA-binding and coiled-coil domains. To gain basic insights into variant disease pathophysiology, we generated two orthologous ASD-associated *fkh-7* missense variants – one harboring a R563G change at the start of the forkhead domain and the other, a R612C change that affects a highly-conserved DNA-binding residue near the middle of the forkhead domain[38]. When challenged with our pheromone-induced dauer formation assay conditions, both missense variants exhibited decreased dauer formation phenotypes that were weaker than the *fkh-7* deletion alleles (Figure 6B,C).

3.4 Discussion

Here, we show that the conserved forkhead box P transcription factor FKH-7/FOXP is required for pheromone-induced diapause entry. We find that larval growth conditions strongly influence *fkh-7* expression and that development through the dauer stages is marked by increasingly stronger and widespread transcription factor expression. FKH-7.a activity in either a subset of chemosensory neurons or the intestine is sufficient to rescue the *fkh-7* mutant dauer formation phenotype, and human FOXP1 can functionally substitute for FKH-7 in this paradigm. Finally, we determine that loss of FKH-7 activity does not result in deformed sensory neuron morphology or alter their positions within the animal's brain. Thus, impaired sensory neuron function in *fkh-7* mutants is likely to stem from physiological deficits.

Advances in gene editing technology have permitted greater access to the genomes of model organisms than ever before. In this study, we've leveraged these new tools to systematically mutagenize precise locations of a conserved, disease-relevant gene. This has enabled us to derive causal relationships between specific *fkh-7* genomic regions and residues with organismal phenotypic severity. The modest dauer formation phenotypes of the missense variants compared to the DBD deletion mutants is interesting because it implies that a smaller subset of FKH-7-mediated gene regulatory networks are impacted in the variants. This can be confirmed by using mRNA-profiling techniques to compare the

differentially-expressed gene profiles between various mutants and potentially lead to identification of key disease-relevant pathways.

In our tissue-specific rescue and GFP reporter expression experiments, we've focused only on the longest predicted transcript *fkh-7*.a. It would be interesting to investigate whether other *fkh-7* transcripts co-express with *fkh-7*.a or are present in different cells entirely. Furthermore, if these different transcripts co-express with *fkh-7*.a, can they functionally substitute for each other in the same behavioral or physiological contexts? The leucine zipper motif is essential for homo- and heterodimerization between FOXP paralogs, which is required for their transcriptional regulatory function[39,40]. Although the FKH-7 coiled-coil domain is conserved to a lesser extent than the DBD, dimerization between different FKH-7 isoforms might mediate some of their functions. If so, this would present another opportunity to study the phenotypic consequences of human disease-relevant coiled-coil domain missense variants using the developmental decision-making paradigm in this study.

3.5 Figures

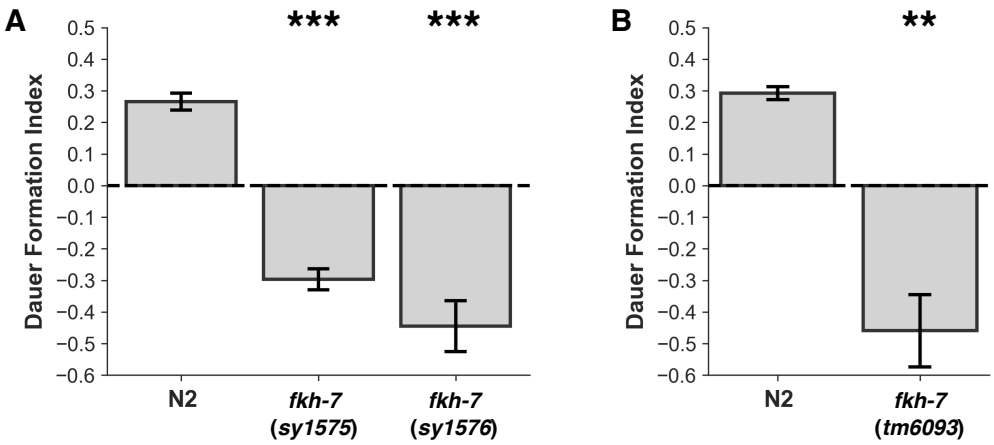

Figure 1. FKH-7 is required for pheromone-induced diapause entry.

(A) Dauer formation assays for 1.26 kb deletion *fkh-7*(*sy1575*) and 1.5 kb deletion *fkh-7(sy1576*) mutants. N=4-5 population assays. Data represented as mean ± SEM, ANOVA followed by Dunnett's compared to N2, ***p<0.001.

(B) Dauer formation assays for *fkh-7*(*tm6093*) mutant. N=3 population assays. Data represented as mean ± SEM, student's t-test equal variance, **p<0.01.

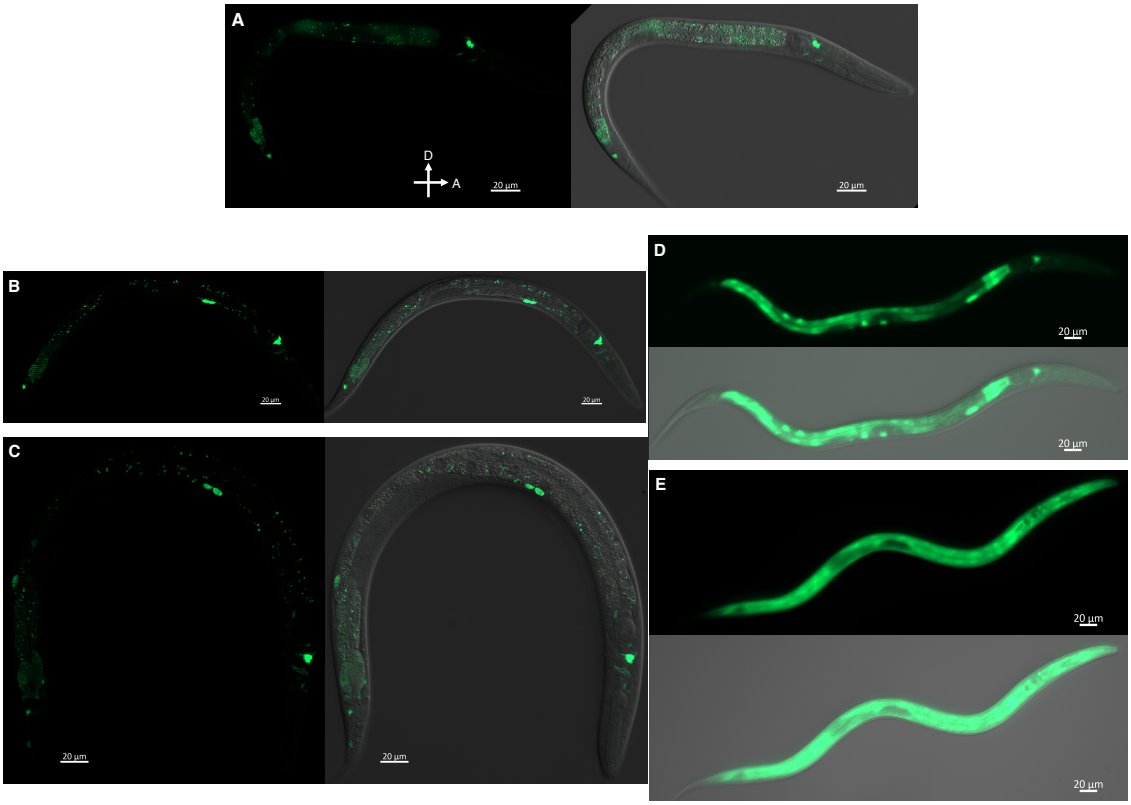

Figure 2. *fkh-7*.a expression pattern during reproductive and dauer development trajectories.

Representative images of P*fkh-7*.a::*GFP* larvae grown under reproductive conditions: (A) L1 stage, (B) L2 stage, (C) L3 stage and pheromone-induced dauer formation conditions: (D) pre-dauer L2d stage, (E) dauer stage.

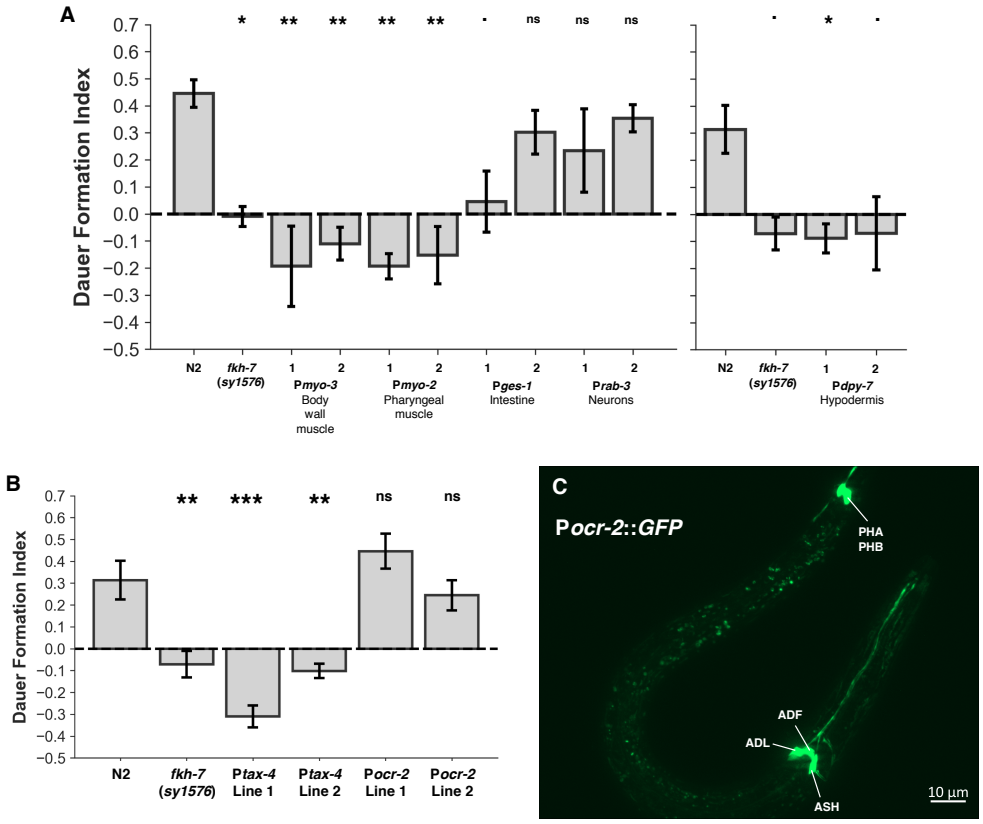

Figure 3. FKH-7.a acts in the nervous system and intestine to promote diapause entry.

(A) Dauer formation assays for tissue-specific *fkh-7*.a cDNA expression in *fkh-7*(*sy1576*) mutants. 2 independent transgenic lines assayed per promoter. N=3-5 population assays, ANOVA followed by Dunnett's compared to N2, ns=no significance, .p<0.1, *p<0.05, **p<0.01.

(B) Dauer formation assays for *fkh-7*.a cDNA expression in *ocr-2* promoter and *tax-4* promoter sensory neuron subsets in *fkh-7*(*sy1576*) mutants. Only transgenic animals counted. N=4 population assays. Data represented as mean ± SEM, ANOVA followed by Dunnett's compared to N2, ns=no significance, **p<0.01, ***p<0.001.

(C) Representative image of P*ocr-2*::*GFP* expression in an L1 stage larva.

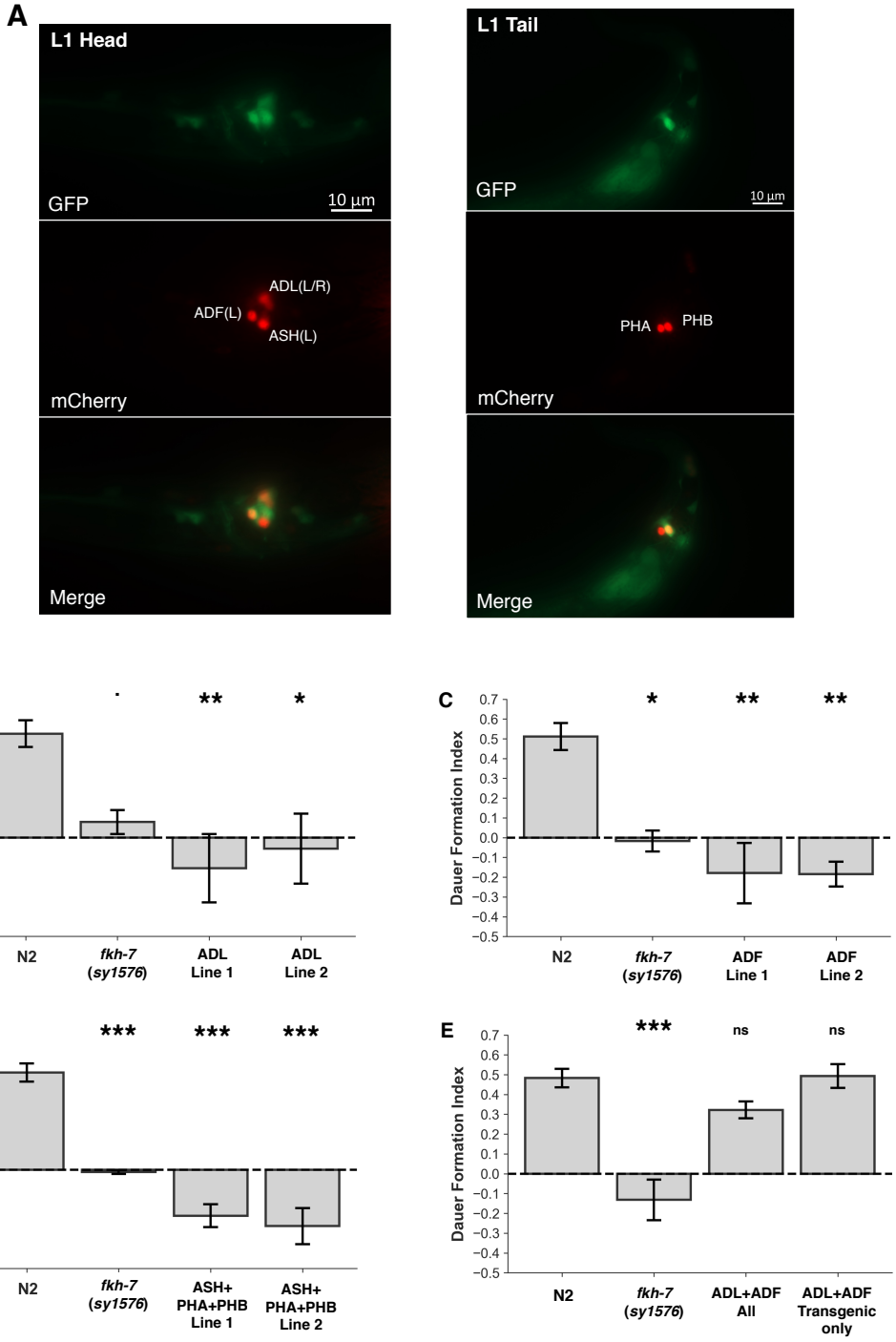
A
L1 Head
GFP
10 µm
ADL(L/R)
ADF(L)
ASH(L)
mCherry
Merge
L1 Tail
GFP
10 µm
PHA
PHB
mCherry
Merge
B
Dauer Formation Index
N2
fkh-7 (sy1576)
ADL Line 1
ADL Line 2
C
Dauer Formation Index
N2
fkh-7 (sy1576)
ADF Line 1
ADF Line 2
D
Dauer Formation Index
N2
fkh-7 (sy1576)
ASH+ PHA+PHB Line 1
ASH+ PHA+PHB Line 2
E
Dauer Formation Index
N2
fkh-7 (sy1576)
ADL+ADF All
ADL+ADF Transgenic only
ns

Figure 4. FKH-7 regulates ADL and ADF neuron function during developmental decision-making.

(A) Representative image of P*fkh-7*.a::*GFP* colocalization with nuclear-localized P*ocr-2*::*mCherry-H2B* in an L1 stage larva head (left) and tail (right).

(B) Dauer formation assays for ADL-specific *fkh-7*.a cDNA expression in *fkh-7*(*sy1576*) mutants. N=3-6 population assays. Data represented as mean ± SEM, ANOVA followed by Dunnett's compared to N2, .p<0.1, *p<0.05, **p<0.01.

(C) Dauer formation assays for ADF-specific *fkh-7*.a cDNA expression in *fkh-7*(*sy1576*) mutants. N=4 population assays. Data represented as mean ± SEM, ANOVA followed by Dunnett's compared to N2, *p<0.05, **p<0.01.

(D) Dauer formation assays for ASH+PHA+PHB-specific *fkh-7*.a cDNA expression in *fkh-7*(*sy1576*) mutants. N=4 population assays. Data represented as mean ± SEM, ANOVA followed by Dunnett's compared to N2, ***p<0.001.

(E) Dauer formation assays for ADL+ADF-specific *fkh-7*.a cDNA expression in *fkh-7*(*sy1576*) mutants. N=3-4 population assays. Results for all animals and transgenic animals only shown. Data represented as mean ± SEM, ANOVA followed by Dunnett's compared to N2, ns=no significance, ***p<0.001.

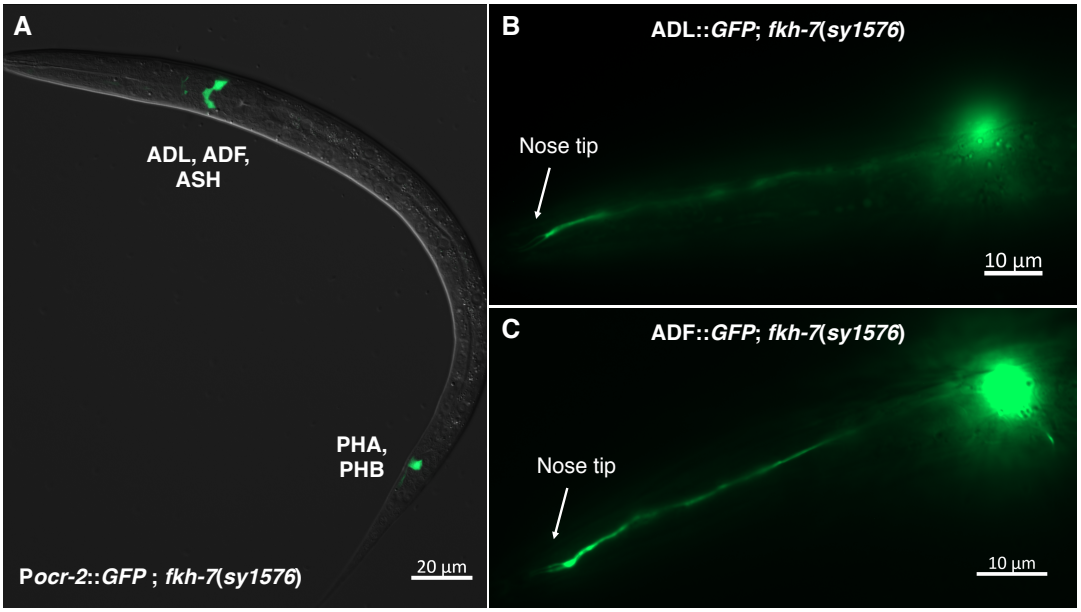

Figure 5. Loss of FKH-7 activity does not disrupt sensory neuron morphology or spatial localization.

(A) Representative image of *fkh-7*(*sy1576*); P*ocr-2*::*GFP* expression in an L1 stage larva.

(B) Representative image of ADL::*GFP* ciliated endings in L2 stage *fkh-7*(*sy1576*) mutants.

(C) Representative image of ADF::*GFP* ciliated endings in L2 stage *fkh-7*(*sy1576*) mutants.

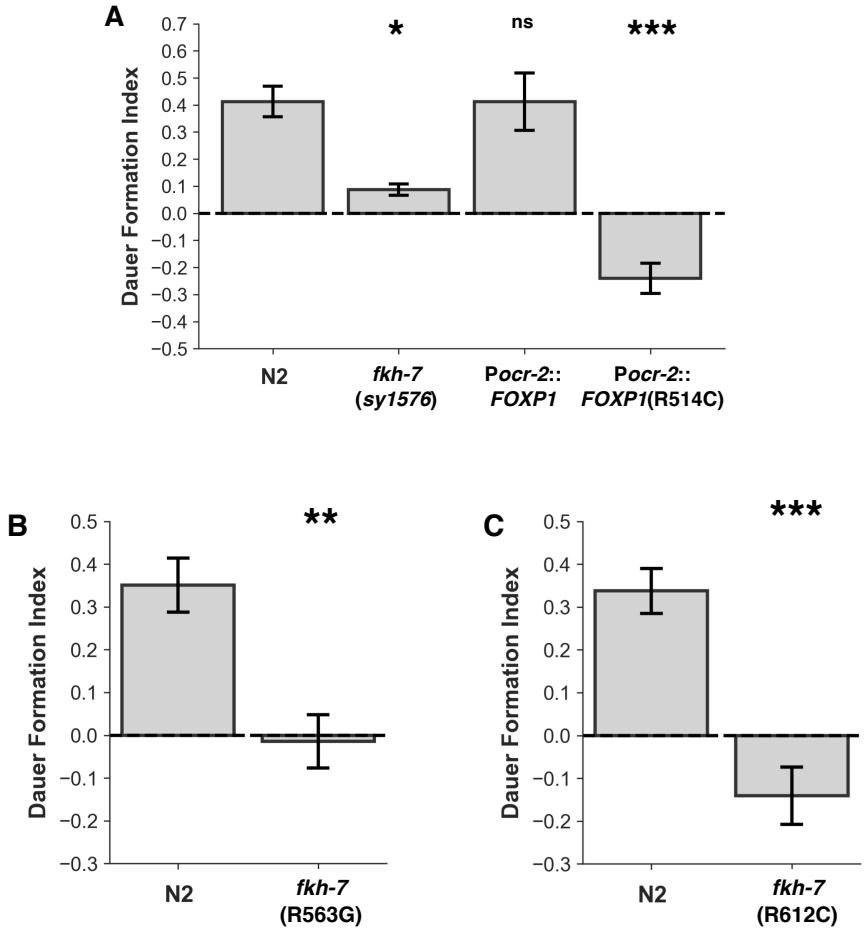

Figure 6. ASD-associated *fkh-7* missense variants have a reduction in dauer formation phenotype.

(A) Dauer formation assays for *ocr-2* promoter-driven *H. sapiens FOXP1* cDNA and *FOXP1*(R514C) cDNA expression in *fkh-7*(*sy1576*) mutants. N=4-5 population assays. Data represented as mean ± SEM, ANOVA followed by Dunnett's compared to N2, ns=no significance, *p<0.05, ***p<0.001.

(B) Dauer formation assays for *fkh-7*(R563G) mutant. N=8 population assays. Data represented as mean ± SEM, student's t-test equal variance, **p<0.01.

(C) Dauer formation assays for *fkh-7*(R612C) mutant. N=5-6 population assays. Data represented as mean ± SEM, student's t-test equal variance, ***p<0.001.

3.6 Materials and Methods

Animal maintenance and strains

Animals were cultivated at 21°C on standard nematode growth media (NGM) plates seeded with *Escherichia coli* OP50 cultured in Luria-Bertani(LB) broth. The following strains were used in this study:

N2 (Bristol)

PS7375: *fkh-7*(*sy1575*)

PS7376: *fkh-7*(*sy1576*)

PS7377: *fkh-7*(*tm6093*)

PS8063: *fkh-7*(*sy906*)

PS8065: *fkh-7*(*sy1316*)

PS8880: *syIs722*[P*fkh-7*.a::*GFP*, P*ocr-2*::*mCherry-H2B*, P*ofm-1*::*RFP*]

PS8610: *syEx1740*[P*rab-3*::*fkh-7.a* cDNA::SL2::*GFP*, P*ofm-1*::*RFP*]; *fkh-7*(*sy1576*)

PS8611: *syEx1741*[P*rab-3*::*fkh-7.a* cDNA::SL2::*GFP*, P*ofm-1*::*RFP*]; *fkh-7*(*sy1576*)

PS8612: *syEx1742*[P*myo-2*::*fkh-7.a* cDNA::SL2::*GFP*, P*ofm-1*::*RFP*]; *fkh-7*(*sy1576*)

PS8613: *syEx1743*[P*myo-2*::*fkh-7.a* cDNA::SL2::*GFP*, P*ofm-1*::*RFP*]; *fkh-7*(*sy1576*)

PS8614: *syEx1744*[P*myo-3*::*fkh-7.a* cDNA::SL2::*GFP*, P*ofm-1*::*RFP*]; *fkh-7*(*sy1576*)

PS8615: *syEx1745*[P*myo-3*::*fkh-7.a* cDNA::SL2::*GFP*, P*ofm-1*::*RFP*]; *fkh-7*(*sy1576*)

PS8616: *syEx1746*[P*ges-1*::*fkh-7.a* cDNA::SL2::*GFP*, P*ofm-1*::*RFP*]; *fkh-7*(*sy1576*)

PS8617: *syEx1747*[P*ges-1*::*fkh-7.a* cDNA::SL2::*GFP*, P*ofm-1*::*RFP*]; *fkh-7*(*sy1576*)

PS8618: *syEx1748*[P*dpy-7*::*fkh-7.a* cDNA::SL2::*GFP*, P*ofm-1*::*RFP*]; *fkh-7*(*sy1576*)

PS8619: *syEx1749*[P*dpy-7*::*fkh-7.a* cDNA::SL2::*GFP*, P*ofm-1*::*RFP*]; *fkh-7*(*sy1576*)

PS8620: *syEx1750*[P*tax-4*::*fkh-7.a* cDNA::SL2::*GFP*, P*ofm-1*::*RFP*]; *fkh-7*(*sy1576*)

PS8621: *syEx1751*[P*tax-4*::*fkh-7.a* cDNA::SL2::*GFP*, P*ofm-1*::*RFP*]; *fkh-7*(*sy1576*)

PS8622: *syEx1752*[P*ocr-2*::*fkh-7.a* cDNA::SL2::*GFP*, P*ofm-1*::*RFP*]; *fkh-7*(*sy1576*)

PS8623: *syEx1753*[P*ocr-2*::*fkh-7.a* cDNA::SL2::*GFP*, P*ofm-1*::*RFP*]; *fkh-7*(*sy1576*)

PS8878: *syEx1753*[P*ocr-2*::*H. sapiens FOXP1* cDNA::SL2::*GFP*, P*ofm-1*::*RFP*]; *fkh-7*(*sy1576*)

PS8913: *syEx1775*[P*ocr-2*::*H. sapiens FOXP1(R514C)* cDNA::SL2::*GFP*, P*ofm-1*::*RFP*]; *fkh-7*(*sy1576*)

PS8923: *syEx1781*[P*sre-1*::*fkh-7.a* cDNA::SL2::*GFP*, P*ofm-1*::*RFP*]; *fkh-7*(*sy1576*)

PS8924: *syEx1782*[P*sre-1*::*fkh-7.a* cDNA::SL2::*GFP*, P*ofm-1*::*RFP*]; *fkh-7*(*sy1576*)

PS9216: *syEx1882*[P*srh-142*::*fkh-7.a* cDNA::SL2::*GFP*, P*ofm-1*::*RFP*]; *fkh-7*(*sy1576*)

PS9217: *syEx1883*[P*srh-142*::*fkh-7.a* cDNA::SL2::*GFP*, P*ofm-1*::*RFP*]; *fkh-7*(*sy1576*)

PS9218: *syEx1884*[P*osm-10*::*fkh-7.a* cDNA::SL2::*GFP*, P*ofm-1*::*RFP*]; *fkh-7*(*sy1576*)

PS9219: *syEx1885*[P*osm-10*::*fkh-7.a* cDNA::SL2::*GFP*, P*ofm-1*::*RFP*]; *fkh-7*(*sy1576*)

PS8980: *syEx1799*[P*sre-1*::*fkh-7.a* cDNA::SL2::*GFP*, P*sre-1*::*fkh-7.a* cDNA::SL2::*GFP,* P*ofm-1*::*RFP*]; *fkh-7*(*sy1576*)

PS8795: *syIs692*[P*ocr-2*::*GFP*]

PS8911: *syIs692*[P*ocr-2*::*GFP*]; *fkh-7*(*sy1576*)

PS9210: *syEx1878*[P*sre-1*::*GFP,* P*ofm-1*::*RFP*]; *fkh-7*(*sy1576*)

PS9211: *syEx1879*[P*srh-142*::*GFP,* P*ofm-1*::*RFP*]; *fkh-7*(*sy1576*)

Molecular biology and transgenesis

*fkh7.*a cDNA was PCR amplified from N2 cDNA library. *H. sapiens FOXP1* cDNA and *FOXP1*(R514C) cDNA synthesized by Integrated DNA Technologies gBlocks. Promoters were PCR amplified from N2 genomic DNA library. Constructs were inserted into pSM *GFP* or pSM *mCherry-H2B* vector backbone using HiFi Assembly or restriction cloning.

Transgenic strains were generated by microinjection of plasmids with co-injection markers into adult worms. Plasmids were injected at 5-50 ng/uL. Co-injection marker P*ofm-1*::*RFP* was injected at 40 ng/uL. 1 kb DNA ladder was used as a filler to bring final DNA concentration to 200 ng/uL.

CRISPR mutagenesis

The PS8063: *fkh-7*(*sy906*) and PS8065: *fkh-7*(*sy1316*) ASD-associated missense variants were generated using CRISPR gene editing as described in Wong *et al.* 2019[41]. The

PS7375: *fkh-7*(*sy1575*) and PS7376: *fkh-7*(*sy1576*) deletion mutants were generated using a CRISPR co-conversion strategy as described in Arribere *et al.* 2014[42].

Pheromone-induced dauer formation assays

Crude dauer pheromone extract was obtained as described in Schroeder and Flatt 2014[43]. Heat-killed OP50 was made by washing bacteria from an overnight culture with virgin S-basal, resuspending with virgin S-basal, and killing at 95-100°C. The afternoon before experiments, L4 worms were picked from well-fed stock plates onto seeded plates and grown overnight at 21°C. Pheromone of desired volume was placed at the center of 35 mm Petri dishes and 2 mL of NGM agar without peptone was poured into each plate. Plates were dried overnight on benchtop at 21°C. On the day of experiments, pheromone plates were seeded with 2 uL heat-killed OP50 and adults animals were allowed to lay 60-70 eggs or 120 eggs (rescue experiments) per plate. Adults were then picked off and 18 uL of heat-killed OP50 added to the plates. Once food has completely dried, plates were parafilmed and placed in 25.5°C incubator for 72 hours. The number of dauers and non-dauers per plate were counted and the Dauer Formation Index (DFI) per plate calculated using the following formula:

$$\text{DFI} = \frac{\text{No. of Dauers} - \text{No. of Non-dauers}}{\text{No. of Dauers} + \text{No. of Non-dauers}}$$

Extrachromosomal array lines that had 70-90% array transmission rates were selected for population assays. All animals on each plate were counted unless noted otherwise. At least 3 population assays were completed for each control and genotype/treatment, with each assay containing 60-70 or 120 worms (*fkh-7*.a rescue experiments). Control and genotype/treatment plates were always assayed simultaneously under the same conditions for comparisons. All statistical analyses were performed in R Studio.

Microscopy

Animals were immobilized with 100 mM sodium azide on 2% agarose pads. Slides were imaged under a ZEISS Imager.Z2 microscope attached to a Axiocam 506 mono camera capture source. Images were processed using ZenPro software.

3.7 References

1. Shimeld, S. M., Degnan, B. & Luke, G. N. Evolutionary genomics of the Fox genes: Origin of gene families and the ancestry of gene clusters. *Genomics* (2010). doi:10.1016/j.ygeno.2009.08.002
2. Halasi, M. & Gartel, A. L. FOX(M1) News - It is cancer. *Molecular Cancer Therapeutics* (2013). doi:10.1158/1535-7163.MCT-12-0712
3. Yu, S., Shao, L., Kilbride, H. & Zwick, D. L. Haploinsufficiencies of FOXF1 and FOXC2 genes associated with lethal alveolar capillary dysplasia and congenital heart disease. *Am. J. Med. Genet. Part A* (2010). doi:10.1002/ajmg.a.33378
4. Chang, S. W. *et al.* Genetic abnormalities in FOXP1 are associated with congenital heart defects. *Hum. Mutat.* (2013). doi:10.1002/humu.22366
5. Takahashi, H., Takahashi, K. & Liu, F. C. FOXP genes, neural development, speech and language disorders. *Adv. Exp. Med. Biol.* (2009). doi:10.1007/978-1-4419-1599-3_9
6. Mercer, F. & Unutmaz, D. The biology of FoxP3: AKey player in immune suppression during infections, autoimmune diseases and cancer. *Adv. Exp. Med. Biol.* (2009). doi:10.1007/978-1-4419-1599-3_4
7. Bowers, J. M. & Konopka, G. The role of the FOXP family of transcription factors in ASD. *Disease Markers* (2012). doi:10.3233/DMA-2012-0919
8. Krupczak-Hollis, K. *et al.* The mouse Forkhead Box m1 transcription factor is essential for hepatoblast mitosis and development of intrahepatic bile ducts and vessels during liver morphogenesis. *Dev. Biol.* (2004). doi:10.1016/j.ydbio.2004.08.022
9. Korver, W. *et al.* Uncoupling of S phase and mitosis in cardiomyocytes and hepatocytes lacking the winged-helix transcription factor Trident. *Curr. Biol.* (1998). doi:10.1016/s0960-9822(07)00563-5
10. Wang, B. Foxp1 regulates cardiac outflow tract, endocardial cushion morphogenesis and myocyte proliferation and maturation. *Development* **131**, 4477–4487 (2004).
11. Ang, S. L. & Rossant, J. HNF-3β is essential for node and notochord formation in mouse development. *Cell* (1994). doi:10.1016/0092-8674(94)90522-3
12. Weinstein, D. C. *et al.* The winged-helix transcription factor HNF-3 beta is required for notochord development in the mouse embryo. *Cell* (1994).
13. Ao, W., Gaudet, J., Kent, W. J., Muttumu, S. & Mango, S. E. Environmentally induced foregut remodeling by PHA-4/FoxA and DAF-12/NHR. *Science (80-.).* (2004). doi:10.1126/science.1102216
14. Hsu, H. T. *et al.* Recruitment of RNA polymerase II by the pioneer transcription factor PHA-4. *Science (80-.).* (2015). doi:10.1126/science.aab1223
15. Updike, D. L. & Mango, S. E. Temporal regulation of foregut development by HTZ-1/H2A.Z and PHA-4/FoxA. *PLoS Genet.* (2006). doi:10.1371/journal.pgen.0020161
16. Gaudet, J. & Mango, S. E. Regulation of organogenesis by the Caenorhabditis elegans FoxA protein PHA-4. *Science (80-.).* (2002). doi:10.1126/science.1065175
17. Kenyon, C., Chang, J., Gensch, E., Rudner, A. & Tabtiang, R. A C. elegans mutant that lives twice as long as wild type. *Nature* (1993). doi:10.1038/366461a0

18. Lin, K., Dorman, J. B., Rodan, A. & Kenyon, C. daf-16: An HNF-3/forkhead family member that can function to double the life-span of Caenorhabditis elegans. *Science (80-.).* (1997). doi:10.1126/science.278.5341.1319
19. Libina, N., Berman, J. R. & Kenyon, C. Tissue-Specific Activities of C. elegans DAF-16 in the Regulation of Lifespan. *Cell* (2003). doi:10.1016/S0092-8674(03)00889-4
20. Zhang, P., Judy, M., Lee, S. J. & Kenyon, C. Direct and indirect gene regulation by a life-extending foxo protein in C. elegans: Roles for GATA factors and lipid gene regulators. *Cell Metab.* (2013). doi:10.1016/j.cmet.2012.12.013
21. Henderson, S. T. & Johnson, T. E. daf-16 integrates developmental and environmental inputs to mediate aging in the nematode Caenorhabditis elegans. *Curr. Biol.* (2001). doi:10.1016/S0960-9822(01)00594-2
22. Murphy, C. T. *et al.* Genes that act downstream of DAF-16 to influence the lifespan of Caenorhabditis elegans. *Nature* (2003). doi:10.1038/nature01789
23. Lai, C. S. L., Fisher, S. E., Hurst, J. A., Vargha-Khadem, F. & Monaco, A. P. A forkhead-domain gene is mutated in a severe speech and language disorder. *Nature* **413**, 519–523 (2001).
24. Horn, D. *et al.* Identification of FOXP1 deletions in three unrelated patients with mental retardation and significant speech and language deficits. *Human Mutation* **31**, (2010).
25. Bacon, C. & Rappold, G. A. The distinct and overlapping phenotypic spectra of FOXP1 and FOXP2 in cognitive disorders. *Human Genetics* (2012). doi:10.1007/s00439-012-1193-z
26. Hamdan, F. F. *et al.* De novo mutations in FOXP1 in cases with intellectual disability, autism, and language impairment. *Am. J. Hum. Genet.* **87**, 671–678 (2010).
27. Haesler, S. *et al.* Incomplete and inaccurate vocal imitation after knockdown of FoxP2 in songbird basal ganglia nucleus area X. *PLoS Biol.* (2007). doi:10.1371/journal.pbio.0050321
28. Bacon, C. *et al.* Brain-specific Foxp1 deletion impairs neuronal development and causes autistic-like behaviour. *Mol. Psychiatry* (2015). doi:10.1038/mp.2014.116
29. DasGupta, S., Ferreira, C. H. & Miesenbock, G. FoxP influences the speed and accuracy of a perceptual decision in Drosophila. *Science (80-.).* **344**, 901–904 (2014).
30. Groschner, L. N., Chan Wah Hak, L., Bogacz, R., DasGupta, S. & Miesenböck, G. Dendritic Integration of Sensory Evidence in Perceptual Decision-Making. *Cell* (2018). doi:10.1016/j.cell.2018.03.075
31. Gerstein, M. B. *et al.* Integrative analysis of the Caenorhabditis elegans genome by the modENCODE project. *Science (80-.).* (2010). doi:10.1126/science.1196914
32. Komatsu, H., Mori, I., Rhee, J. S., Akaike, N. & Ohshima, Y. Mutations in a cyclic nucleotide-gated channel lead to abnormal thermosensation and chemosensation in C. elegans. *Neuron* (1996). doi:10.1016/S0896-6273(00)80202-0
33. Tobin, D. M. *et al.* Combinatorial expression of TRPV channel proteins defines their sensory functions and subcellular localization in C. elegans neurons. *Neuron* **35**, 307–318 (2002).
34. Bargmann, C. I. & Horvitz, H. R. Control of larval development by chemosensory neurons in Caenorhabditis elegans. *Science (80-.).* (1991). doi:10.1126/science.2006412

35. Schackwitz, W. S., Inoue, T. & Thomas, J. H. Chemosensory neurons function in parallel to mediate a pheromone response in C. elegans. *Neuron* **17**, 719–728 (1996).
36. Ware, R. W., Clark, D., Crossland, K. & Russell, R. L. The nerve ring of the nematode Caenorhabditis elegans: Sensory input and motor output. *J. Comp. Neurol.* (1975). doi:10.1002/cne.901620106
37. Boyle, A. P. *et al.* Comparative analysis of regulatory information and circuits across distant species. *Nature* (2014). doi:10.1038/nature13668
38. Sollis, E. *et al.* Identification and functional characterization of de novo FOXP1 variants provides novel insights into the etiology of neurodevelopmental disorder. *Hum. Mol. Genet.* **25**, 546–557 (2016).
39. Li, S., Weidenfeld, J. & Morrisey, E. E. Transcriptional and DNA Binding Activity of the Foxp1/2/4 Family Is Modulated by Heterotypic and Homotypic Protein Interactions. *Mol. Cell. Biol.* (2004). doi:10.1128/mcb.24.2.809-822.2004
40. Chae, W. J., Henegariu, O., Lee, S. K. & Bothwell, A. L. M. The mutant leucine-zipper domain impairs both dimerization and suppressive function of Foxp3 in T cells. *Proc. Natl. Acad. Sci. U. S. A.* (2006). doi:10.1073/pnas.0600225103
41. Wong, W. R. *et al.* Autism-Associated missense genetic variants impact locomotion and neurodevelopment in Caenorhabditis elegans. *Hum. Mol. Genet.* (2019). doi:10.1093/hmg/ddz051
42. Arribere, J. A. *et al.* Efficient marker-free recovery of custom genetic modifications with CRISPR/Cas9 in caenorhabditis elegans. *Genetics* (2014). doi:10.1534/genetics.114.169730
43. Schroeder, N. E. & Flatt, K. M. In vivo imaging of Dauer-specific neuronal remodeling in C. elegans. *J. Vis. Exp.* e51834 (2014). doi:10.3791/51834

CHAPTER 4: Concluding remarks

In the course of studying the basic neurobiology underlying *C. elegans* development, I have revealed how interneurons contribute to larval developmental plasticity and discovered a novel neuronal function for an evolutionarily-conserved, disease-relevant transcription factor in developmental decision-making.

However, there are clearly still many questions left to be explored along these fascinating lines of research. For instance, how many other neuropeptides contribute to this decision-making process? By identifying these neuropeptides and their cognate receptors through functional screening, their neuronal site(s) of action can subsequently be traced through gene expression analysis. This will lead to a comprehensive view of the neural architecture mediating *C. elegans* developmental plasticity. Furthermore, what are the molecular pathways mediated by FKH-7 in the sensory neurons identified in this work and how do they go awry when FKH-7 function is perturbed? The application of single-cell transcriptomics is poised to deliver such answers.

In vivo studies on animal development can be challenging because of the longer assay timescales and correspondingly complex mixture of variables that can affect data quality and interpretation. But the result of such efforts is a rewarding glimpse of how our own biology came to be, through the lens of a dissecting microscope staring down into a tiny worm.